NACA RM L57K26

NACA

RESEARCH MEMORANDUM

BEHAVIOR OF SOME MATERIALS AND SHAPES IN SUPERSONIC FREE JETS AT STAGNATION TEMPERATURES UP TO 4,210° F, AND DESCRIPTIONS OF THE JETS

By E. M. Fields, Russell N. Hopko, Robert L. Swain,
and Otto F. Trout, Jr.

Langley Aeronautical Laboratory
Langley Field, Va.

NATIONAL ADVISORY COMMITTEE
FOR AERONAUTICS

WASHINGTON
February 24, 1958
Declassified February 8, 1960

NACA RM L57K26

NATIONAL ADVISORY COMMITTEE FOR AERONAUTICS

RESEARCH MEMORANDUM

BEHAVIOR OF SOME MATERIALS AND SHAPES IN SUPERSONIC FREE JETS AT STAGNATION TEMPERATURES UP TO 4,210° F, AND DESCRIPTIONS OF THE JETS

By E. M. Fields, Russell N. Hopko, Robert L. Swain, and Otto F. Trout, Jr.

SUMMARY

This report presents the results of some tests of a number of materials and shapes in two supersonic free jets at stagnation temperatures up to about 4,210° F.

Some of the tests were conducted in a supersonic chemical jet at stagnation temperatures up to 4,210° F, and other tests were conducted in a ceramic-heated air jet at stagnation temperatures up to 4,150° F.

The test results are presented in the form of enlargements of selected frames from motion pictures made during tests of aluminum alloy, copper, Inconel, magnesium, mild steel, molybdenum, stainless steel, titanium, alumina (Al_2O_3), zirconia (ZrO_2), graphite, bakelite, and nylon. The stagnation temperatures for these tests ranged from 1,950° F to 4,210° F.

The results of these exploratory tests indicate that graphite, zirconia, and a material made of alternate layers of molybdenum and zirconia had high resistance to the heating conditions. Melting was delayed by increasing nose bluntness and accelerated by adding holes and grooves in the models near the stagnation point.

Descriptions of the jets are included in appendixes to the report.

INTRODUCTION

The increasing emphasis on flight at very high speeds in the earth's atmosphere has resulted in pressing needs for information on the behavior of materials and body shapes subjected to high-temperature environments

and high heating rates that result from the high flow velocities. Although simultaneous simulation of temperature, testing medium, and time duration of the test is difficult, much information may be obtained by using welding torches, shock tubes, radiant heaters, and rocket-motor jets. The rocket jet is, at present, one of the most widely used testing devices and provides considerable information. The major limitation of a rocket-motor jet as a high-temperature testing device appears to be the jet composition, which is usually different from that of air.

The Langley Pilotless Aircraft Research Division has in operation a supersonic chemical jet, which is a rocket-motor free jet (2.1-inch exit diameter) having an exit Mach number of about 2.6 and stagnation temperatures up to about 4,200° F. This jet is composed of steam, nitrogen, and either hydrogen or oxygen. This Division has also developed and put into operation a ceramic-heated jet (laboratory model), which is a high-temperature testing facility using heated air as the testing medium. (See ref. 1.) In this facility the air is heated as it passes through a preheated bed of zirconia (ZrO_2) spheres, and the air is then exhausted to the atmosphere as an 0.79-inch-diameter free jet at $M \approx 2$ and at stagnation temperatures up to about 4,150° F. Descriptions of the jets are included in appendixes A and B.

The present report contains some data on the behavior of a few materials and body shapes tested in the two jets soon after they became operative. The qualitative resistance of the test bodies to severe aerodynamic heating and thermal shock was determined from 16-millimeter motion pictures of the tests.

SYMBOLS

GENERAL

d	diameter of nose hemisphere, ft
h	heat-transfer parameter, Btu/(sq ft)(sec)(°F)
M	Mach number
$\dot{m}$	mass-flow rate, lb/sec
R	ratio of red fuming nitric acid to ammonia by weight
$r = d/2$	

T_s stagnation temperature, °F

t time, measured from time at which model reaches center of jet, sec

t_m time at which visible melting starts, sec

γ ratio of specific heats

CHEMICAL

CO carbon monoxide

H_2 hydrogen

H_2O steam

N_2 nitrogen

O_2 oxygen

TEST FACILITIES

The tests reported herein were made in two of the high-temperature ground test facilities of the Langley Pilotless Aircraft Research Division. One of the facilities is the supersonic chemical jet, which consists of an acid-ammonia rocket-motor free jet. The other is the ceramic-heated jet (laboratory model), hereinafter referred to as the hot-air jet. A description of the chemical jet is included as appendix A, and the ceramic-heated jet is described in appendix B.

The chemical jet uses red fuming nitric acid and ammonia as propellants and produces a 2.1-inch-diameter axisymmetric free jet with a maximum flow velocity of about 7,400 feet per second ($M \approx 2.6$) and a maximum stagnation temperature of about 4,200° F. The chemical-jet test medium is approximately one-half superheated steam, the remainder being made up of nitrogen and hydrogen or nitrogen and oxygen, depending on the fuel mixture ratio.

In the hot-air jet, compressed air is passed through a preheated bed of zirconia spheres and then through a $M \approx 2$ axisymmetric nozzle

having exit conditions of about 14 to 15 lb/sq in. abs static pressure, 105 lb/sq in. abs stagnation pressure, and stagnation temperatures up to about 4,150° F.

In both jets the model is mounted on a quick-acting device which moves the model into the jet after supersonic flow has been established. It takes about 0.03 to 0.05 second for the model to move from the edge of the jet to the center.

The aerodynamic heating rate in the chemical jet is from 30 percent to 80 percent higher than that of the hot-air jet, because of the difference in Mach number and jet composition.

PRESENTATION AND INTERPRETATION OF TEST RESULTS

The test results are presented in figures 1 to 19. The pictures shown in this report are enlargements of frames from 16-millimeter motion pictures of the tests. Some were taken with color film at 133 frames per second, and others were taken with black and white film at 500 frames per second. Zero time ($t = 0$) corresponds to the time when the model centers in the jet.

Table I shows the pertinent test conditions for models tested in the chemical jet. Table II presents a summary of materials behavior during the present tests.

Inasmuch as the hot-air jet uses air as the test medium, results from this test facility are applicable to high-speed flight in the atmosphere. A large part of the chemical-jet test medium is superheated steam, and the effects of this steam on oxidation-prone materials for the present tests are not known. In the chemical jet, where the jet was composed of steam (H_2O), nitrogen (N_2), and hydrogen (H_2), the test medium is referred to as "reducing" since only minute traces of free oxygen (O_2) are theoretically present. Equilibrium jet compositions were computed taking into account the dissociation of some components at the higher jet temperatures. The descriptive word "reducing" is used to define only the general nature of the exhaust stream and hence is enclosed in quotation marks. Although materials tests in the hot-air jet and the chemical jet cannot be directly correlated at present, the chemical jet has many specialized applications such as in the investigation of the effects of shape variation for a given material and in the investigation of materials behavior for specialized environments (for example, jet vanes immersed in the rocket jet). The chemical jet can also be used for cooling tests in which oxidation of the surface material is not an important factor.

In a number of tests the gases surrounding the model or in the wake were hot enough to give the appearance of flames, and such an occurrence is referred to as "burning" or "luminosity" in the text and table II. There was some loss of detail in photographic reproduction and as a result only the most vigorous "burning" can be seen in the figures (see, for example, model 25 at $t = 4.74$ and 5.17 in fig. 1 and model 19, $t = 0.23$ and 0.38 in fig. 3).

ACCURACY

The accuracy in determining when an event occurs during a test is dependent on three factors:

(1) Accuracy of the electronic timing reference

(2) Accuracy of determining when the model is centered in the jet

(3) Accuracy of identification of start of event under consideration

The timing errors in factor (1) are negligible. The error in factor (2) is generally less than 0.01 second, and the error in factor (3) depends on the type of event being considered. For example, the breaking away of part of the model can be determined to within 0.002 to 0.004 second. The time to start melting for a material such as stainless steel, which becomes plastic and does not run freely when melting, may be in error by as much as 0.05 or 0.06 second. In general, the values shown in this report for time to start melting are believed to be accurate to within ± 0.03 or 0.04 second. The accuracy is believed to be within the limits of repeatability between nominally identical tests. Some of the test-condition uncertainties are discussed in appendixes A and B.

MODELS

Sketches of the models are shown as part of the figures containing the test results (figs. 1 to 19). Dimensions shown are in inches. The shapes tested were generally axisymmetric cone-cylinders, hemisphere-cylinders, or hemisphere-cones.

DISCUSSION

CHEMICAL-JET TESTS

Materials Behavior

Aluminum alloy, mild steel, stainless steel, and titanium.- Figure 1 shows the behavior of aluminum alloy (2024-T), mild steel (SAE 1010), stainless steel (type 347), and titanium (Ti-75) in the chemical jet at a stagnation temperature of 3,990° F to 4,020° F. During destruction both the aluminum alloy and stainless steel flowed sluggishly and burned in the wake. The mild steel melted and flowed freely but no burning could be seen. The titanium burned vigorously with a brilliant white flame originating at the surface and extending for some distance downstream. The burning of the aluminum alloy and titanium was intermittent at first and grew steady, but remained intermittent for the stainless steel. Flaking and scaling of the stainless-steel surface could be seen near the end of the test.

All the models shown in figure 1 were the same size and shape, although the lighting makes models 24 and 25 appear to be slimmer than the others.

The titanium started burning without prior melting, and it is assumed that melting began with the appearance of burning at $t = 3.38$ seconds.

Molybdenum.- Figure 2 shows molybdenum (of unknown composition, but thought to be commercially pure) being tested at stagnation temperatures of 3,660° F and 4,200° F in the chemical jet in a "reducing" atmosphere (steam, N_2, H_2). The model was a nozzle-throat insert from a discarded rocket. Several sources in the literature state that molybdenum oxidizes "rapidly" at high temperatures, and it was of interest to see how well it stood up in a test medium that contained essentially no free oxygen. Models 37 and 40 are actually a single piece tested twice. The first test (model 37) at 3,660° F for about 12 seconds heated the molybdenum white-hot and caused a slight amount of surface melting. Later the same piece was tested again (model 40) at 4,200° F, and considerable destruction of the molybdenum resulted.

During the later stages of the test for model 37, the wake became slightly luminous, and the luminous region soon attached itself to the rear of the molybdenum where molten metal could be seen. No general burning of the metal surface could be seen. Model 40 showed similar behavior except for considerable luminosity at the front end early in

the test. The model was not altered or refinished between tests, and the second test was run after the model had cooled to room temperature.

Molybdenum has a melting temperature of about 4,700° F, and the reason for the slight surface melting at stagnation temperatures of 3,660° F and 4,200° F is not known. It may be that the steam, upon coming into contact with the hot molybdenum surface, liberated free oxygen which reacted with the molybdenum and part of the heat of oxide formation heated the molybdenum surface to its melting temperature. The oxidation of 1 pound of molybdenum to molybdenum trioxide (MoO_3) liberates enough heat to melt about 6.5 additional pounds of molybdenum.

It is not believed that the molten metal observed was molten MoO_3 (melting point approximately 1,430° F). Limited experience (not reported) with the formation of MoO_3 has shown it to be highly volatile at and above its melting temperature; when the molybdenum was heated in still air, the MoO_3 formed a fluffy white crystalline structure and no molten surface was observed, and when the molybdenum was heated in a slowly flowing medium, neither the crystalline structure nor a molten surface was observed as the molybdenum slowly disappeared.

Magnesium.- Figure 3 shows the behavior of magnesium (AZ31B) in the chemical jet. Model 19 was a magnesium rod in a bakelite holder and was tested at a stagnation temperature of 3,820° F. The tip of the magnesium began melting in 0.15 second, and immediately the melting area and wake began burning vigorously with an intense white flame. The burning appeared to originate at or very close to the melting surface, and the magnesium was rapidly consumed.

Copper.- Figure 4 shows the behavior of commercially pure copper in the chemical jet. Model 11 was a copper cone with a $\frac{1}{8}$-inch-radius hemisphere tip and a 0.076-inch-diameter hole along the axis of symmetry but closed at the back end to simulate a missile total-pressure orifice. Shortly after the test began, the copper nose began drooping slowly because of partial failure of the model support, and the resulting angle of attack was about 5° at the end of the test. Motion pictures of this test did not show any burning at the copper surface or in the wake.

Inconel.- Figure 5 shows the behavior of Inconel hemisphere-cylinder shells in the chemical jet, tested at stagnation temperatures of 3,040° F and 3,150° F. Motion pictures of these tests did not show any burning at the Inconel surface or in the wake.

Alumina.- Figure 6 shows the behavior of alumina (Al_2O_3) in the chemical jet at a stagnation temperature of 3,440° F. Model 34 was a hollow cylinder closed at the front end and was made by cutting off the

closed end of a commercial thermocouple well having a melting temperature of 3,600° F. A large crack appeared suddenly at about 0.6 second and the piece broke up along this crack at about 0.7 second, ending the test.

Graphite.- Shown in figure 7 is the behavior of graphite in the chemical jet.

Model 35 was a solid hemisphere-cylinder of graphite (National Carbon Company, AGR graphite), tested in a "reducing" jet (steam, N_2, H_2) at a stagnation temperature of 3,140° F. At the end of the test (about 9 seconds) only minor erosion was evident. The surface was smoothed with sandpaper and run again (pictures not shown) in a reducing jet for about 8 seconds at a stagnation temperature of 3,670° F, and again only minor erosion resulted.

Calculations of the available energy at 2,700° F show that the necessary conditions are present for the "water-gas" reaction (combination of steam and carbon to form H_2 and CO), and the minor erosion experienced for the graphite may have been due largely to this chemical activity.

Bakelite.- Figure 7 also shows the behavior of bakelite in the chemical jet. Model 38 in figure 7 was a solid hemisphere-cylinder cut from a thick slab of bakelite reinforced with cellulose fabric and was tested at a stagnation temperature of 3,770° F. The planes of the reinforcing fabric were normal to the model axis of symmetry.

The softening temperature of the bakelite resin is about 400° F, but during the test the surface of the model charred and eroded rather slowly. This somewhat surprising behavior of low-melting bakelite is considered to be due to its low thermal conductivity (0.004 that of steel and 0.0008 that of aluminum at low temperature) and a possibly beneficial surface reaction at high temperature. It has been suggested that perhaps the carbon in the resin forms a porous erosion barrier at the bakelite surface when the material is subjected to high-speed high-temperature flows. It may be also that gaseous products, formed at the surface by breakdown of the resin, are ejected into the boundary layer and thus act as a coolant.

Zirconia.- Figure 8 shows the behavior of a zirconia sphere in the chemical jet. Model 9 was a zirconia sphere placed on the end of a slender stainless-steel cone, tested at a stagnation temperature of 2,850° F. The sphere was the same as those used as heat exchangers in the hot-air jet (see appendix B) and the main purpose of the test was to see if the sphere would withstand moderate thermal shock. No damage

to the sphere could be detected during the heating cycle. The zirconia sphere protected the cone tip to some extent, since a blunter stainless-steel cone (lower heat transfer) at a lower temperature began melting in a time less than the duration of this test (see model 13, fig. 9). The zirconia, although not tested at higher temperatures, appeared to have good resistance to thermal shock.

Zirconia-molybdenum.- Model 39 in figure 8 was made up of an outer shell of alternate layers of zirconia and molybdenum flame-sprayed on a mild-steel rod. The multilayered coating was about 1/8 inch thick and contained a total of 18 layers (9 of each material), the outermost layer being zirconia. This model had been tested previously at 3,500° F in the chemical jet (pictures not shown) for about 10 seconds with negligible damage, and the present test at a stagnation temperature of 4,210° F (model 39) was the second test for this piece. The first damage to model 39 became visible when a small chip came off the hemisphere near the stagnation area at 7.6 seconds. A larger chip came off at 10 seconds and the test was terminated at 11.4 seconds. Motion pictures of the test show that the edges of the damaged area eroded very slowly. The purpose of the layers of molybdenum was to reduce the severity of the thermal shock effects by acting as a relatively strong binder between the zirconia layers. The multilayered model was not repaired or smoothed between tests.

Nylon.- Figure 9 shows the results of a test using a nylon rod as a possible cooling device. The movies of the test show a film spreading rapidly from front to rear on the stainless-steel holder as the test starts, and it is assumed that this film comes from the gaseous nylon condensing on the holder. As soon as the nylon-rod base decomposed enough to expose the edge of the hole in the stainless-steel holder, the edge of the hole heated rapidly. Motion pictures of these tests did not show any visible melting or burning.

Shape Effects

Grooved flat-face cylinders.- Figure 10 shows the behavior of three flat-face mild-steel (SAE 1010) cylinders in the chemical jet at stagnation temperatures of 3,580° F to 3,660° F. The purpose of these tests was to determine the effect of grooves in the flat face on the time to start melting, and it can be seen (fig. 10(b)) that the grooves drastically hastened the onset of visible melting. The angle of attack of model 31 increased slowly throughout the test because of partial failure of the model support sleeve. These tests were run in a "reducing" atmosphere (steam, N_2, H_2).

Nose bluntness.- Figure 11 shows the behavior of two stainless-steel (type 347) cones at a stagnation temperature of about 2,625° F

(±5° F) in the chemical jet. Models 13 and 14 differed only in the nose hemisphere radius, and the sharper cone began melting first, as would be expected from the higher theoretical stagnation-point heat-transfer rates for the sharper cone (ref. 2). Both models had a hole (closed at the back end) along the longitudinal axis to simulate a total-pressure orifice.

Airplane-like shape.- Figure 12 shows the behavior of two identical stainless-steel (type 347) airplane-like configurations at stagnation temperatures of 3,870° F (model 26) and 4,190° F (model 27). The notches in the wing leading edges were caused by severe local heating of undetermined origin. It can be seen that model 26 suffered a more rapid destruction than model 27 although model 26 was tested at a lower stagnation temperature, and it is believed that the difference in oxygen content of the test medium was a principal factor.

It may be noted in figure 12 (see model 26, t = 6.7) that the canopy remains relatively cool during the test, and the wing-body juncture appeared to be somewhat cooler than the adjacent fuselage and wing area.

Model surface colors indicate the relative temperature levels. The last photograph (t = 9.75) for model 26 shows the remains of the fuselage breaking away from the support.

HOT-AIR-JET TESTS

General

The stagnation temperature of the hot-air jet decreases during a run as the hot sphere bed gives up heat to the testing air. The stagnation temperatures shown for the hot-air jet are the temperatures of the zirconia spheres at the top of the bed at the beginning of the test and about 1 minute after the end of the test. Limited tests with thermocouples in the jet at about 2,000° F have shown that the air stagnation temperature appears to be somewhat lower (perhaps as much as 100° F) than the temperature of the top of the bed, but further calibration will be necessary to establish the relationship between the air stagnation temperature and bed temperature. Test results from the hot-air jet are applicable to flight in the atmosphere, but correlation between test results in the chemical jet and flight in the atmosphere is at present uncertain.

Materials Behavior

Titanium.- Model 60, shown in figure 13, was a titanium (Ti-75) cone slightly blunted with a small (0.032-inch) radius hemisphere, and destruction (bursts of flame) began in slightly less than 1 second. Intermittent bursts of flame appeared in the wake near the cone tip before any melting could be seen and immediately enveloped the entire model. A similar cone (pictures not shown) with a sharp tip behaved in a similar manner at a stagnation temperature of 3,960 to 3,600° F except that the sharp tip could be seen to melt slightly before burning started.

Aluminum alloy.- Figure 14 shows the behavior of an aluminum-alloy (2024-T) hemisphere-face cone (model 52) in the hot-air jet at stagnation temperatures of 2,050° F to 1,950° F. Other tests (not shown) of identical models at stagnation temperatures up to 4,000° F show similar behavior. The metal flowed rather sluggishly as it melted, in comparison with steel. No burning could be seen at the model surface or in the wake for any of these models.

Although the timing for model 52 was not reliable and no quantitative results were obtained, pictures of this model have been included to show the general behavior of aluminum at a stagnation temperature of about 2,000° F.

Mild steel, stainless steel, and graphite.- Figure 15 shows the behavior of mild steel (SAE 1010), stainless steel (type 347), and graphite (National Carbon Company, AGR graphite) at stagnation temperatures of about 3,850° F to 4,100° F in the hot-air jet. All models were 90° apex-angle cones.

The graphite (model 67) was practically undamaged after about 19 seconds of testing. The stainless steel (model 72) began melting in about 9 seconds, and the mild steel (model 73) began melting in about 3 seconds. The stainless steel showed an intermittent flame in the wake beginning at about 9.5 seconds, and the flame became steady at about 10.5 seconds. The flames for models 72 and 73 appeared to originate at or near the melting surface, and droplets of molten metal were blown off during the later stages of the test.

Zirconia-molybdenum.- Figure 16 shows the results from tests of a multilayered hemisphere-cylinder model at a stagnation temperature of 3,920° to 3,460° F in the hot-air jet. Model 59 had been tested previously in the chemical jet at 3,500° F for about 10 seconds (pictures not shown), and in the hot-air jet at stagnation temperatures of 3,980° to 3,400° F for about 18 seconds (pictures not shown) and about 11 seconds at 4,210° F in the chemical jet as model 39. (See fig. 8.) During the test at 3,920° F (model 59) in the hot-air jet a small flake came

off the nose immediately after centering in the jet and a steady shower of sparks came from the stagnation area for a short period thereafter. The sparks probably indicated the breakup of a part of a zirconia layer.

The test identified as model 59 shows the appearance of this multilayered model after a cumulative testing time of about 1 minute at stagnation temperatures between 3,400° F and 4,210° F. From these limited tests it appears that a multilayer type of construction of these materials has good resistance to thermal shock.

Magnesium.- Figure 17 shows the behavior of magnesium (AZ31B) in the hot-air jet at stagnation temperatures of about 3,160° F to 2,950° F (±10° F). Model 74 was a sharp cone (10° total angle) and models 75, 76, 77, and 78 were blunted with hemisphere tips at about 80 percent, 60 percent, 40 percent, and 20 percent, respectively, of the original length. Very soon after the magnesium began melting, the wake began burning brightly starting at a point slightly downstream of the cone. The wake burning was at first intermittent but generally became stronger and steadier and appeared to attach to the melting surface during the later stages of the tests.

Shape Effects

Nose bluntness.- Figure 18(b) shows the time to start melting plotted against nose radius for the magnesium models shown in figure 17. Also included in figure 18 are the results for four magnesium cones (models 68, 69, 70, 71; pictures not shown) at the same stagnation temperature but having flat faces instead of hemispheres. Once the flat-face cones began melting, their behavior was similar to that of the hemisphere-faced cones. It may be seen in figure 18(b) that for a given nose radius the flat-face cones began melting later than the hemisphere-faced cones. The curves were drawn through $t = 0$ because the sharp-tip cone (model 74) had started melting by the time it was centered in the jet.

Surface irregularities.- Figure 19 shows the results of some tests in the hot-air jet to determine some effects of nose surface irregularities. Models 61 to 66 were solid mild-steel (SAE 1010) cones blunted with a 1/8-inch-radius hemisphere tip and were tested at a stagnation temperature of about 4,020° F to 3,600° F. Five of the noses were disfigured with holes or grooves and the time to start melting for each is indicated and can be compared with the time for the smooth nose (model 61). The results show that a hole at or near the stagnation point caused the nose to start melting before the plain nose, probably because of the high surface-to-volume ratio at the edges of the holes. Similar results were noted for grooves in flat-face models in the chemical jet (see fig. 8), but the effects of the grooves on the flat-face models were

much more pronounced. It may be noted in figure 19 that the plain nose (model 61) started melting before model 65 although both models had smooth stagnation areas, and no explanation for this lack of repeatability can be offered at present. The edges of the hole in the side of model 65 apparently did not melt and were covered by molten metal from the stagnation area during the latter part of the test. Model 66 (groove around hemisphere) began melting before the smooth-nose model, but the motion pictures of the test do not show whether the groove area or the stagnation area began melting first.

The holes in the models were three-dimensional depressions made by a drill or sharp-end punch.

CONCLUDING REMARKS

In the present report two new high-temperature supersonic free jets are described. These free jets are useful for testing the behavior of materials and shapes at stagnation temperatures up to about 4,200° F. Pictures of some exploratory tests of materials and shapes in these high-temperature free jets are shown.

Graphite, zirconia, and a material composed of alternate flame-sprayed layers of molybdenum and zirconia showed good resistance to high-temperature supersonic flow and thermal shock.

Cones blunted with hemisphere tips required longer times to start melting than sharp cones, and the time to start melting increased with increased hemisphere radius. Flat-face cones took longer to start melting than hemisphere-face cones having the same nose radius.

Hemisphere-tip cones and flat-face cylinders, with surface disfigurements in the stagnation area, began melting earlier than smooth models. The grooves in the flat-face cylinders had a more pronounced effect on the time to start melting than did the holes in the hemisphere-tip cones.

Several materials showed luminosity near the surface or in the wake while melting. When magnesium melted, the model wake was strongly luminous. The wake of titanium during destruction showed very strong luminosity amounting to a general conflagration.

Langley Aeronautical Laboratory,
National Advisory Committee for Aeronautics,
Langley Field, November 7, 1957.

APPENDIX A

SUPERSONIC CHEMICAL JET

GENERAL

The supersonic chemical jet of the Langley Pilotless Aircraft Research Division is a modified liquid-fuel rocket system of the general type employed in the Gorgon missile. Anhydrous liquid ammonia and red fuming nitric acid (14 percent nitrogen dioxide) are mixed in the presence of a small amount of alkali catalyst (lithium) and burned, yielding a supersonic stream of high-temperature combustion products. This high-temperature supersonic stream is used to test the behavior of materials and aerodynamic configurations at high stagnation temperatures and pressures.

A simplified flow diagram of the facility and a photograph of the chemical-jet motor are shown as figure 20, and the calculated jet-flow parameters are shown in figures 21 and 22. The rocket motor is regeneratively cooled by the nitric acid before the acid enters the combustion chamber, yielding an essentially adiabatic combustion system. The models are mounted on a quick-acting model inserter which is actuated by an air-powered hydraulic cylinder, the action of which may be electrically programed. The model mount may be adapted to accommodate models up to 1 inch in diameter.

The selection of the liquid-ammonia—red-fuming-nitric-acid propellant combination resulted from four main considerations: (1) a transparent jet which would permit good photographic coverage and visual observation during test, (2) the self-igniting nature of the propellant combination in the presence of an alkali catalyst, (3) excellent system-development history, and (4) reasonable range of mixture-ratio control without occurrence of combustion instability.

JET PROPERTIES

Theoretical

The jet is 2.1 inches in diameter at the nozzle exit. The jet properties are varied by changing either the ratio of acid to ammonia or the total mass-flow rate or both. A choice of mixture ratio and total mass flow fixes the stagnation temperature and pressure. The

theoretical interrelation of important jet parameters for this nozzle is shown in figure 21.

The maximum theoretical stagnation temperature of about 4,200° F occurs at the stoichiometric mixture ratio, at which ratio the jet is composed mainly of superheated steam, nitrogen, and hydrogen. (See fig. 21(c).) For the lower temperatures, the jet may be either "oxidizing" (steam, N_2, and O_2) if the propellant mixture is acid-rich, or "reducing" (steam, N_2, and H_2) if the propellant mixture is ammonia-rich.

The jet is composed of about one-half superheated steam, with the rest consisting of nitrogen and oxygen, or nitrogen and hydrogen, depending on the propellant-mixture ratio. The jet also contains traces of atomic hydrogen, atomic oxygen, nitric oxide, and the hydroxyl radical. The theoretical jet properties shown in figure 21 were calculated with the assumption of a constant-composition expansion process through the nozzle, with resulting identical compositions at the nozzle exit and in the combustion chamber.

The theoretical heat-transfer coefficients at the stagnation point of a hemisphere in the jet, calculated by the method of references 2 and 3, are shown in figure 22. These values are for laminar flow, and it should be noted that the turbulence level of the jet may be high.

Simplified calculations indicate that the stagnation area of a model located near the jet exit may receive from 3 to 30 Btu/(sq ft)(sec) by radiation at stagnation temperatures of 1,500° to 4,000° F, respectively. This radiation energy was calculated with the assumption that only the water vapor, at about 10 atmospheres partial pressure, was radiating. Total radiation from the nozzle wall, assuming that all the radiant energy is distributed evenly over the surface area of a 1-inch-diameter hemisphere, is about 0.8 Btu/(sq ft)(sec) for maximum temperature conditions. The radiant-heat input to a model stagnation area is negligible except for very blunt noses; for a 1-inch-diameter hemisphere the radiant heat input may be of the order of 4 percent to 5 percent of the aerodynamic heating at the stagnation point.

Actual

Of the jet properties shown in figure 21, only the stagnation (chamber) pressures have been measured to date. The measured values have generally been within 5 percent of the theoretical values, based on the measured propellant flow rates. These differences are due to inefficiencies inherent in the combustion system and are influenced by

injector design, motor design, and nonattainment of combustion-product chemical equilibrium.

It is to be expected that these inefficiencies would be reflected by a decrease in stagnation temperature. The extent of this temperature loss is unknown at present. Also, as the propellant-mixture ratio is changed from the stoichiometric, these inefficiences become larger, especially the inefficiency resulting from nonattainment of chemical equilibrium. The very short residence time of the combustion products in the motor makes the attainment of equilibrium conditions very unlikely. The exhaust jet at highly acid-rich operating conditions has a dirty yellow color, probably resulting from undissociated red fuming nitric acid. Similarly, at very ammonia-rich operating conditions, the exhaust stream has a pronounced white color, probably resulting from undissociated ammonia. The calculated stagnation temperatures at these mixture ratios far removed from the stoichiometric ratio are probably different from the actual temperatures, possibly as much as several hundred degrees Fahrenheit.

Little is known at present regarding the chemical activity of the jet exhaust stream. It is to be expected that reactions occurring at the surface of a model immersed in this stream would differ to some degree from those reactions which would occur on the model if it were tested in an airstream of comparable stagnation temperature and pressure. The high water (steam) content of the exhaust probably influences or catalyzes some surface reactions which would not occur in air, especially on metal test specimens. The extent of the influence of this water is as yet undetermined.

The jet-flow parameters shown for tests in this report are theoretical values based on measured fuel and oxidizer flow rates.

The turbulence level of the jet has not been measured, but may be high because of the necessity of thoroughly mixing the propellants in the combustion chamber.

JET OPERATION

High-pressure nitrogen gas forces the propellants from the tanks, through the system, and into the combustion chamber. The lithium, which is added to the ammonia before it enters the injector, acts as a catalyst to insure smooth starts and even burning when the propellants are mixed in the combustion chamber. The jet may be operated by programed electrical solenoid flow valves or may be operated manually by opening

and closing a single valve which controls both propellant lines simultaneously.

TEST PROCEDURE

The model to be tested is mounted on a quick-acting model inserter. The jet is started and, at a predetermined time, the model is inserted into the exhaust stream. Camera lights, cameras, recorders, and timing devices are all turned on in a preset sequence. A programer permits the complete automation of the test.

During a test, continuous records are made of the motor thrust, propellant flow rates, chamber pressure, propellant tank pressures, and model test duration. The test specimen is photographed on 16-millimeter motion-picture film at 133 frames per second (color) and about 500 frames per second (black and white). Continuous records of thermocouple and pressure measurements may be made.

APPENDIX B

CERAMIC-HEATED JET (LABORATORY MODEL)

GENERAL

The ceramic-heated jet (laboratory model) of the Langley Pilotless Aircraft Research Division provides a $M = 2.0$ supersonic air jet 0.79 inch in diameter, having a maximum stagnation temperature of 4,000° F and a maximum stagnation pressure of 105 lb/sq in. abs. The testing air is passed through a preheated bed of zirconia spheres and emerges through a supersonic nozzle as an axisymmetric free jet with a stagnation temperature essentially that of the top of the preheated bed. The supersonic nozzle is made of stainless steel and is water cooled. The supersonic heated airstream is used to test the behavior of materials and aerodynamic shapes at high stagnation temperatures.

During a test the air stagnation temperature decreases at a rate of 5° to 15° F per second as the preheated zirconia spheres give up heat to the testing air. The jet may be operated continuously, the running time being limited only by the acceptable stagnation-temperature drop during the run. Runs of 100 seconds duration have been made, during which time the temperature of the top of the zirconia sphere bed decreased from about 4,000° F to about 3,300° F.

A simplified sketch and photographs of the facility are shown in figure 23.

JET PROPERTIES

Theoretical

The calculations of the nozzle exit values of temperature, velocity, pressure, and Mach number shown in figure 24 were made with a value of γ (ratio of specific heats) corresponding to the nozzle exit static temperature. Since the exit conditions are a function of γ, a simultaneous iteration process was used to calculate the exit Mach number (from known area ratio) and static temperature. The γ-values thus obtained were then used to calculate the exit velocities and pressures. This process was convenient, and it was felt that the accuracy of the values of the exit conditions was sufficient. A stagnation pressure of 105 lb/sq in. abs was used for the calculations.

The values of stagnation-point laminar heat-transfer parameter $h\sqrt{d}$ shown in figure 24 were calculated by using the modified Sibulkin method (refs. 2 and 3). The values of γ used in calculating the stagnation-point velocity gradient (ref. 3) were obtained by averaging the γ-values for the static temperatures immediately upstream and immediately downstream of the normal shock. Again an iteration procedure was used.

The values of γ for various temperatures were taken from reference 4.

Actual

Stagnation-temperature measurements have been made at temperatures up to 3,000° F by using thermocouples exposed to the flow. Comparison of thermocouple temperatures with bed temperatures obtained with an optical pyrometer show that the stagnation temperature of the jet may be as much as 100° F lower than the top of the bed. No comparisons have been made at higher temperatures. Stagnation temperatures shown in the present report for the jet are the temperatures of the top of the zirconia-sphere bed as measured with an optical pyrometer. The $M = 2.0$ free jet can be operated at any temperature between 1,800° F and 4,000° F. The temperature of 1,800° F was chosen as the lower limit of operation to minimize thermal shock and to prevent excessive shifting of the ceramic parts.

A rough verification of the exit Mach number has been made by measuring the angle of disturbance propagation from the nozzle exit lip from shadowgraphs.

The stagnation pressure of air entering the heated pebble bed is indicated on a visual pressure gage. The stagnation pressure at the top of the bed is indicated on a visual pressure gage and also recorded with an oscillograph.

JET OPERATION AND TEST PROCEDURE

Before a test is made, the zirconia-sphere bed, figure 23(a), is heated to the desired temperature by forcing the products of combustion from the oil burner through the bed from the top to the bottom. The temperature of the top of the bed is determined by using an optical pyrometer focused on the top of the bed through a quartz window in the side of the vessel (fig. 23(c)). The burner uses number 2 fuel oil and air to produce bed temperatures up to 3,200° F; to obtain temperatures

between 3,200° F and 4,000° F the burner air is enriched with oxygen. Maximum output of the burner is 500,000 Btu/hr. The temperature of the bed varies from a maximum at the top to a lower value at the bottom. For example, when the top of the bed is 4,000° F the bottom may be about 800° F. The entire bed is not brought up to the test temperature because to do so would impose severe thermal shock on the zirconia spheres at the bottom of the bed where the cold testing air enters. When the bed is heated to the desired temperature and temperature distribution, the burner is turned off.

The jet is started by introducing air into the bottom of the zirconia-sphere chamber. The test air flows through the hot bed from the bottom to the top and absorbs heat in the process. During the test the model is moved in and out of the jet by remote control by using the model support system shown in figure 23(b). A test is ended by removing the model from the jet and cutting off the high-pressure air supply.

In practice, the temperature of the bed is never allowed to drop below 1,800° F between runs so that thermal shock to the bed and side walls will be minimized during the preheating and testing cycles. During a test the bed temperature drops about 5° to 15° F per second as the hot sphere bed gives up heat to the test air.

DATA RECORDING

Model behavior during testing is recorded on 16-millimeter motion-picture film at 133 and 500 frames per second. Temperatures of the models as measured with thermocouples may be recorded on a high-speed oscillograph (this procedure was not used in the tests reported herein). Pressures on the model and inside the zirconia-sphere chamber may also be recorded on a high-speed oscillograph.

REFERENCES

1. Purser, Paul E., and Hopko, Russell N.: Exploratory Materials and Missile-Nose-Shape Tests in a 4,000° F Supersonic Air Jet. NACA RM L56J09, 1956.

2. Sibulkin, M.: Heat Transfer Near the Forward Stagnation Point of a Body of Revolution. Jour. Aero. Sci. (Readers' Forum), vol. 19, no. 8, Aug. 1952, pp. 570-571.

3. Reshotko, Eli, and Cohen, Clarence B.: Heat Transfer at the Forward Stagnation Point of Blunt Bodies. NACA TN 3513, 1955.

4. Hilsenrath, Joseph, Beckett, Charles W., et al.: Tables of Thermal Properties of Gases. NBS Cir. 564, U. S. Dept. Commerce, 1955.

TABLE I.- CHEMICAL-JET TEST CONDITIONS

Model	Chamber pressure, lb/sq in. gage	R	$\dot{m}$	γ	M	H_2O, percent	N_2, percent	H_2, percent	O_2, percent	T_s, ^oF
3	253	4.30	1.907	1.263	2.70	53.9	28.3	0	17.2	3,150
4	260	4.30	1.918	1.263	2.70	53.9	28.3	0	17.2	3,150
5	258	4.58	1.880	1.268	2.70	52.5	28.0	0	18.8	3,040
7	244	4.42	1.917	1.264	2.70	53.3	28.1	0	17.9	3,100
9	271	5.17	1.796	1.272	2.71	50.0	27.7	0	21.3	2,850
11	258	4.99	1.813	1.270	2.71	50.7	27.8	0	20.9	2,910
13	246	5.91	1.818	1.279	2.72	47.5	27.2	0	24.7	2,630
14	251	5.95	1.822	1.279	2.72	47.5	27.2	0	24.8	2,620
19	314	2.95	1.685	1.245	2.67	61.9	29.6	0	7.5	3,820
24	310	2.64	1.732	1.242	2.66	64.2	30.0	0	4.6	4,020
25	314	2.64	1.733	1.242	2.66	64.2	30.0	0	4.6	4,020
26	318	2.87	1.722	1.244	2.67	62.5	29.8	0	6.9	3,870
27	310	2.38	1.758	1.239	2.66	65.4	30.3	.6	1.9	4,190
31	298	1.64	1.936	1.264	2.70	52.9	29.5	16.7	0	3,660
32	314	1.58	1.894	1.267	2.71	51.5	29.4	18.3	0	3,580
33	305	1.61	1.904	1.266	2.71	52.2	29.5	17.4	0	3,620
34	301	1.48	1.879	1.274	2.72	49.0	29.1	21.2	0	3,440
35	281	1.28	1.889	1.287	2.74	43.5	28.7	27.2	0	3,140
37	312	1.64	1.916	1.264	2.70	52.9	29.5	16.7	0	3,660
38	319	1.73	1.942	1.259	2.69	55.1	29.7	14.2	0	3,770
39	338	2.34	2.072	1.239	2.66	65.5	30.4	1.0	1.5	4,210
40	334	2.12	2.040	1.241	2.66	63.7	30.4	4.8	0	4,200
43	309	2.64	1.993	1.242	2.66	64.2	30.0	0	4.6	4,020
46	304	2.68	1.945	1.242	2.66	63.9	30.0	0	5.0	3,990

TABLE II.- SUMMARY OF MATERIALS BEHAVIOR DURING EXPLORATORY TESTS

Material	Facility	Approximate T_s, °F	Figures	Remarks
Aluminum alloy (2024-T)	Chemical jet	4,000	1	Flowed sluggishly while melting and cooled rapidly. Wake generally luminous.
	Hot-air jet	2,000	14	Behavior same as in chemical jet except wake not luminous.
Copper (commercially pure)	Chemical jet	2,900	4	Melted and ran freely.
Inconel	Chemical jet	3,100	5	Flowed sluggishly while melting. No apparent luminosity in wake.
Magnesium (AZ31B)	Chemical jet	3,800	3	Strong luminosity in wake and at or near metal surface. Luminosity became visible shortly after melting started.
	Hot-air jet	3,000	17	Same behavior as in chemical jet.
Mild steel (SAE 1010)	Chemical jet	4,000	1	Molten metal flowed freely and cooled slowly. Some luminosity near surface and in wake for test in reducing jet but not for oxidizing jet.
	Hot-air jet	4,100	15	Molten metal flowed freely. Luminosity visible near melting surface.
Molybdenum (composition unknown but believed to be commercially pure)	Chemical jet	3,700 and 4,200	2	Jet was "reducing" (steam, H_2, N_2). Slight surface melting; faint luminosity near melting surface.
Stainless steel (type 347)	Chemical jet	4,000	1	Some luminosity near surface. When melting lasted for several seconds, a thick scale formed on the surface and was blown off or ejected in fairly large chunks.
	Hot-air jet	4,100	15	Some luminosity near surface. Drops of molten netal blown off during test. No scaling visible.
Titanium (Ti-75)	Chemical jet	4,000	1	Strong luminosity near surface and in wake, amounting to a violent conflagration.
	Hot-air jet	2,900	13	Same behavior as in chemical jet.
Alumina (Al_2O_3)	Chemical jet	3,400	6	Broke up in less than 1 second, apparently from thermal shock.
Zirconia (ZrO_2)	Chemical jet	2,800	8	No apparent reaction.
Zirconia-molybdenum	Chemical jet	4,200	8	Slow erosion and good thermal shock resistance.
	Hot-air jet	3,900	16	Same behavior as in chemical jet.
Graphite (National Carbon Co., AGR)	Chemical jet	3,100	7	Slow erosion and good thermal shock resistance.
	Hot-air jet	4,100	15	Same behavior as in chemical jet.
Bakelite	Chemical jet	3,800	7	Slow erosion.
Nylon	Chemical jet	3,100	9	Fairly rapid destruction; appeared to give some protection to steel holder.

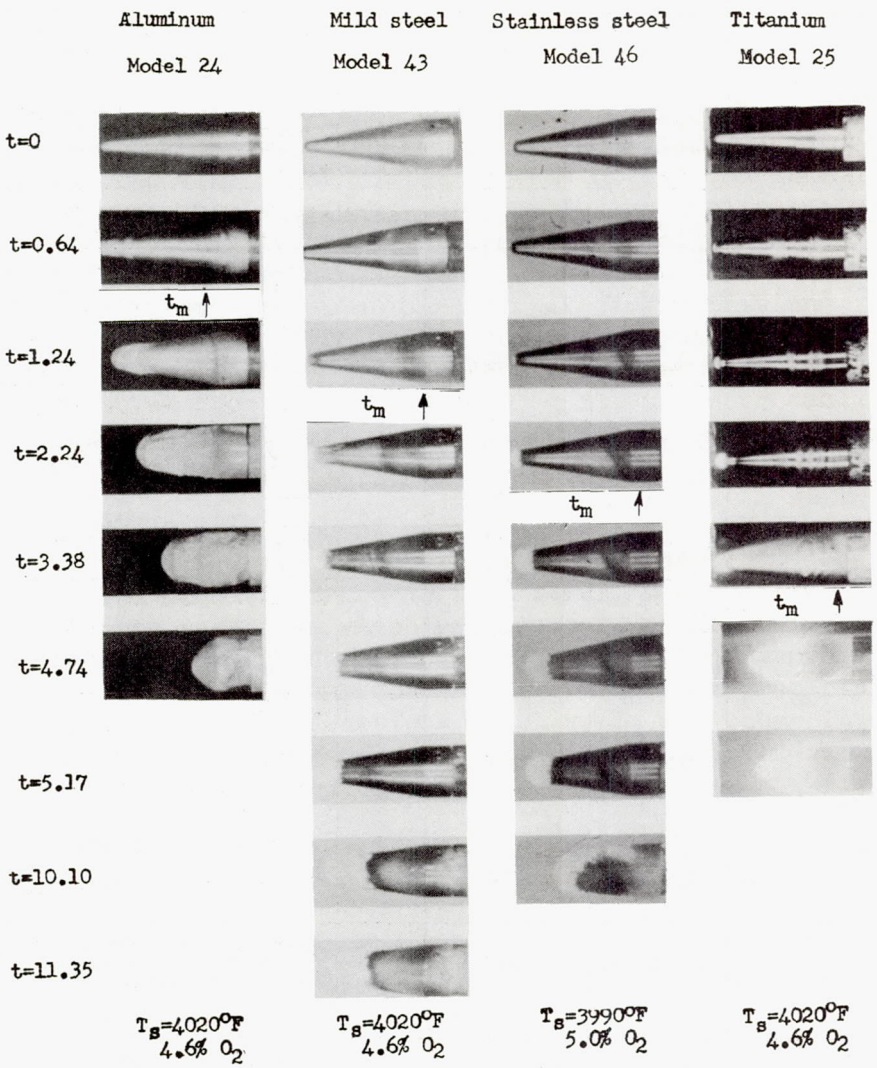

Figure 1.- Behavior of aluminum-alloy, mild-steel, stainless-steel, and titanium cones in chemical jet.

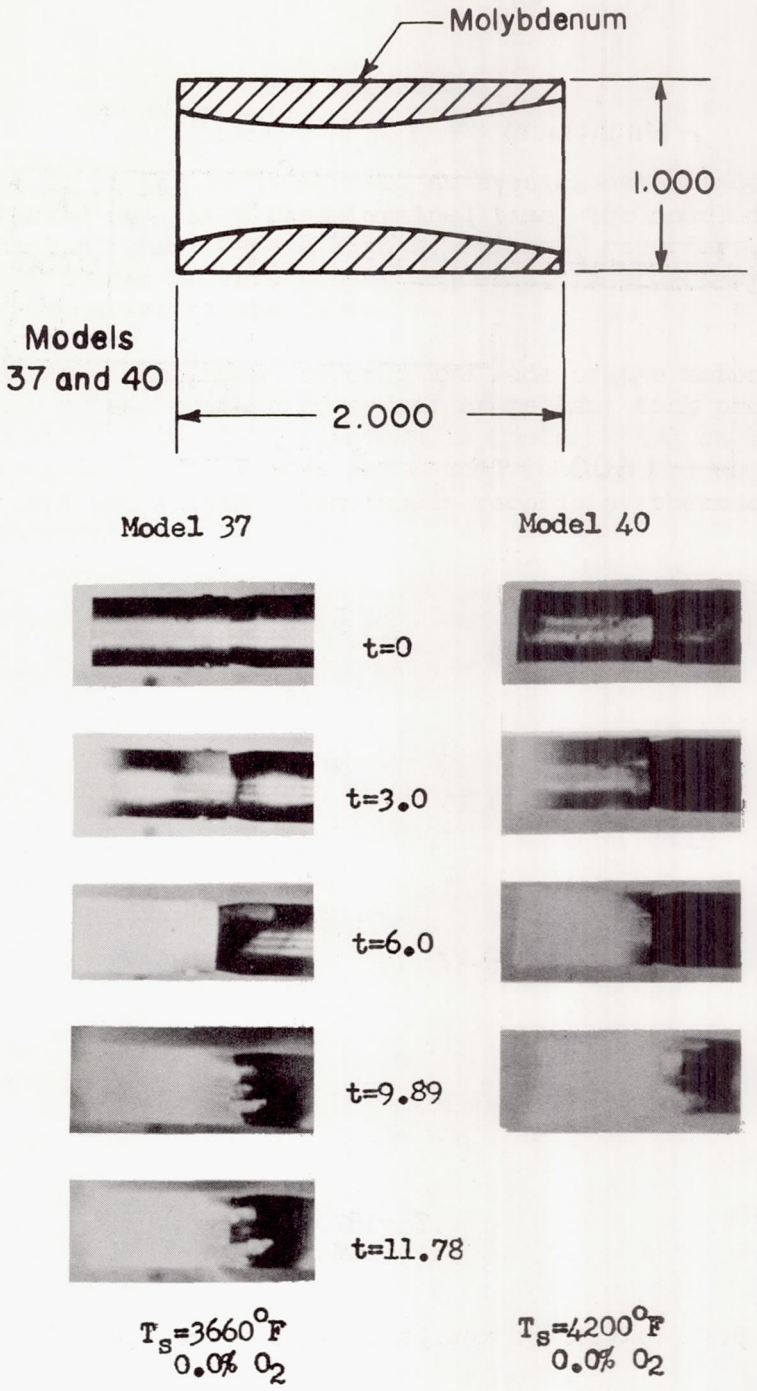

Figure 2.- Behavior of molybdenum in chemical jet. L-57-4423

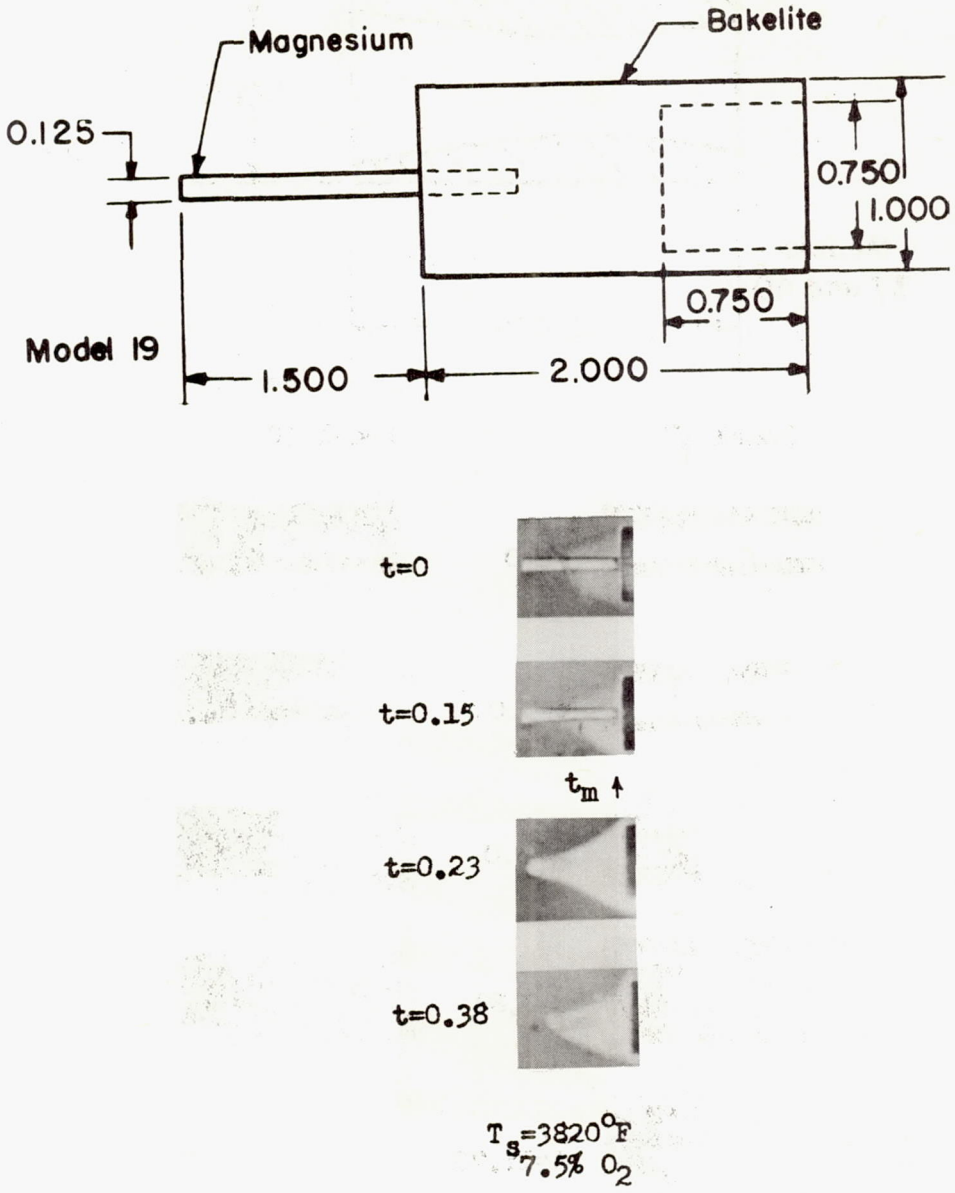

Figure 3.- Behavior of magnesium in chemical jet. L-57-4424

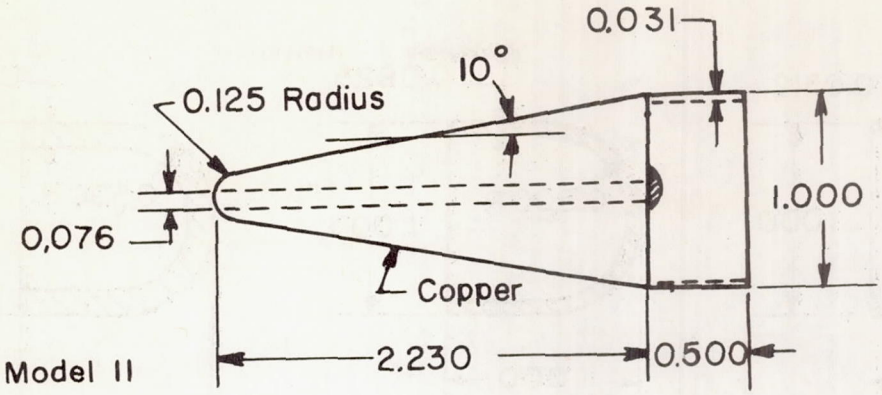

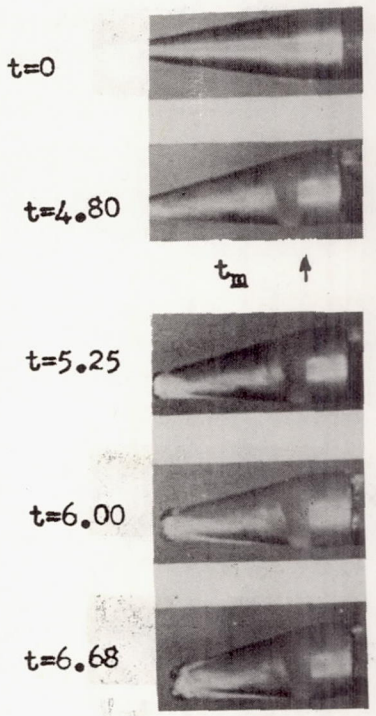

T_s=2910°F
20.9% O_2

Figure 4.- Behavior of copper in chemical jet. L-57-4425

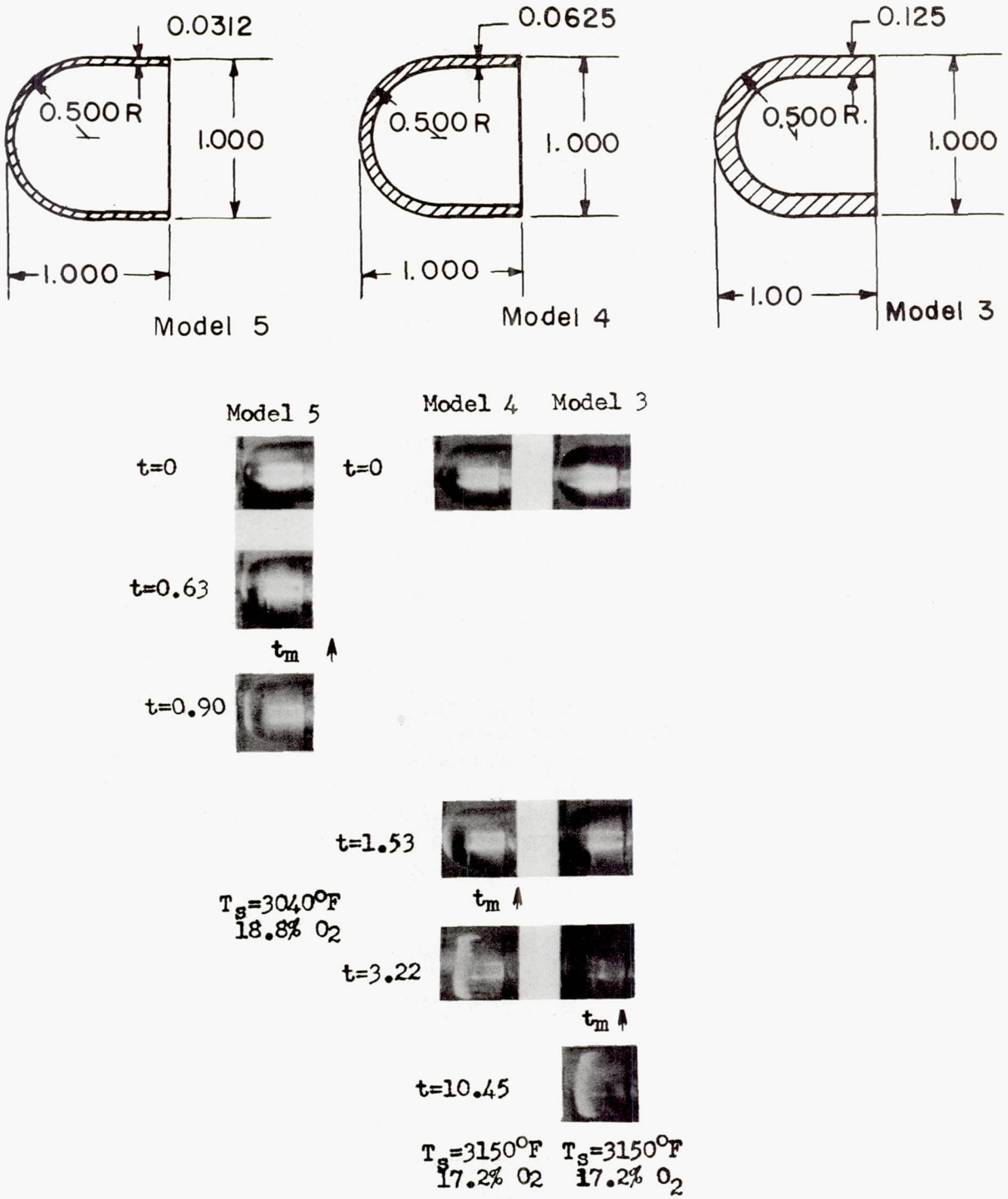

L-57-4426

Figure 5.- Behavior of Inconel thin shell models in chemical jet.

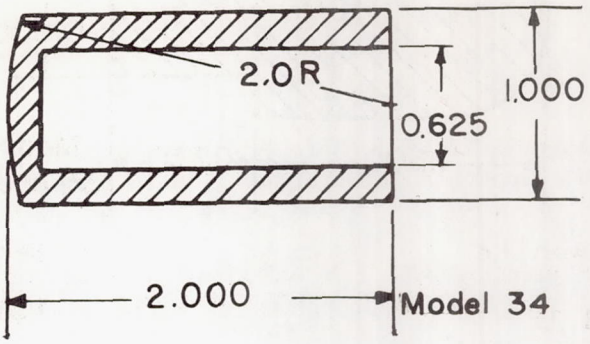

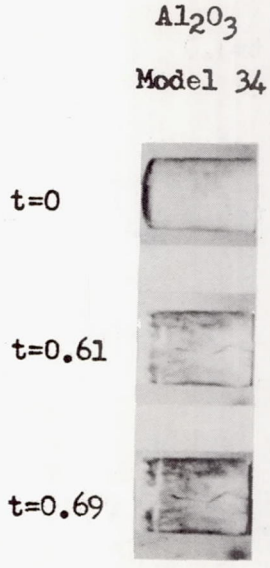

L-57-4427

Figure 6.- Behavior of alumina (Al_2O_3) in chemical jet.

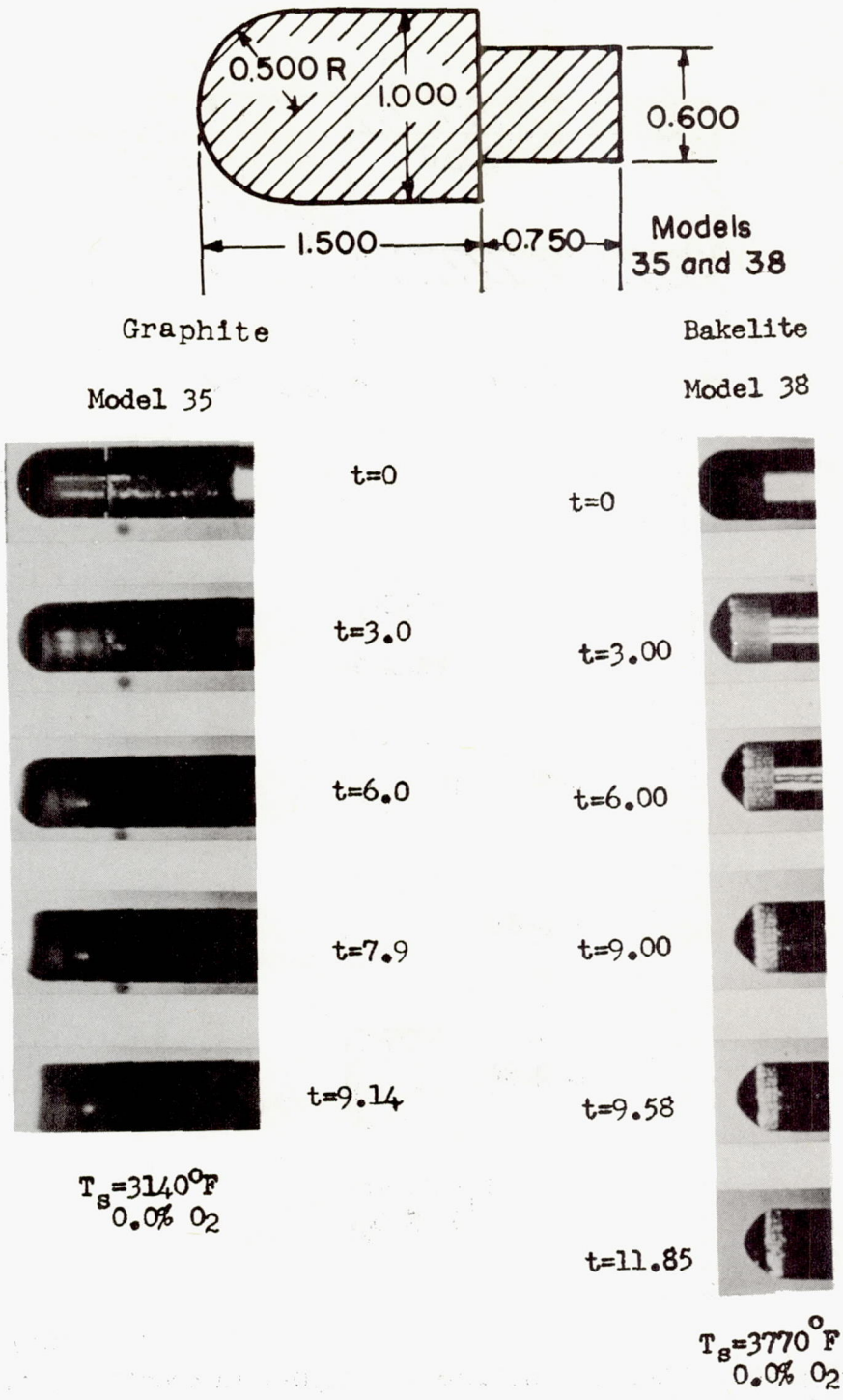

L-57-4428

Figure 7.- Behavior of graphite and bakelite in chemical jet.

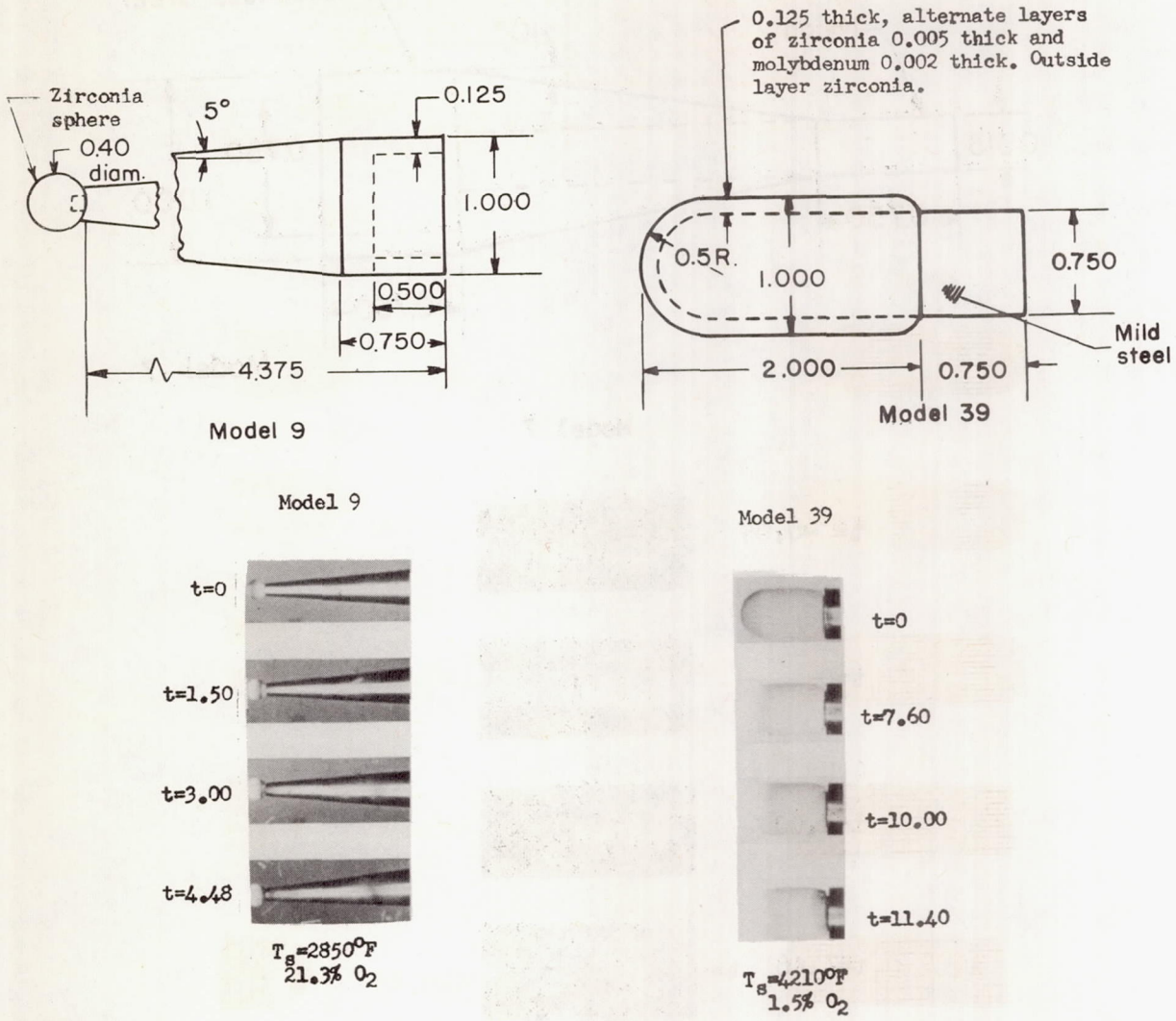

L-57-4429

Figure 8.- Behavior of zirconia and multilayered zirconia-molybdenum in chemical jet.

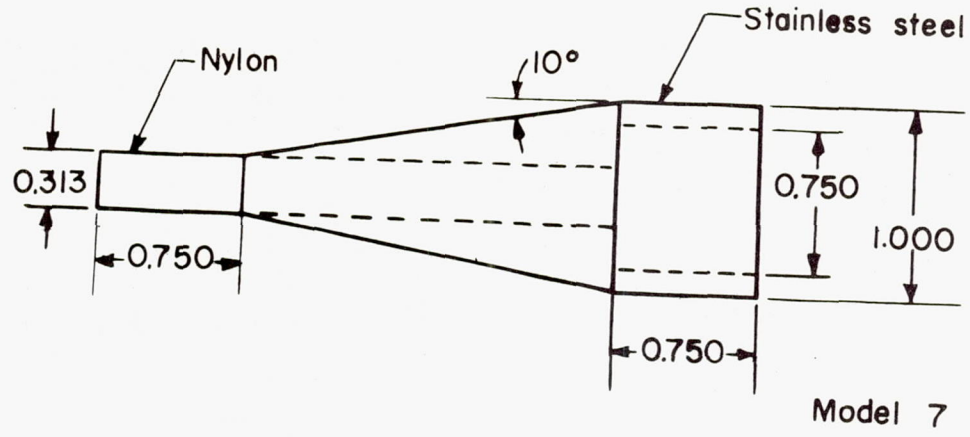

Model 7

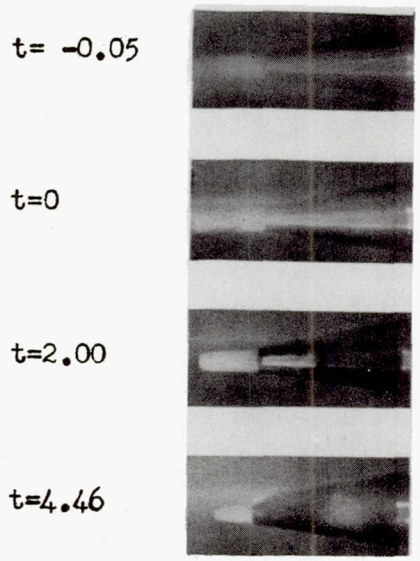

T_s=3100°F
17.9% O_2

Figure 9.- Behavior of nylon in chemical jet. L-57-4430

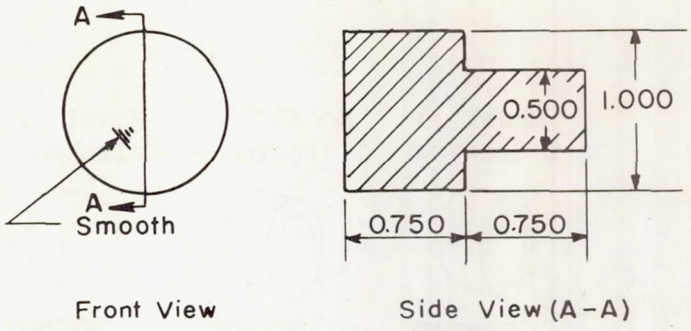

Model 31

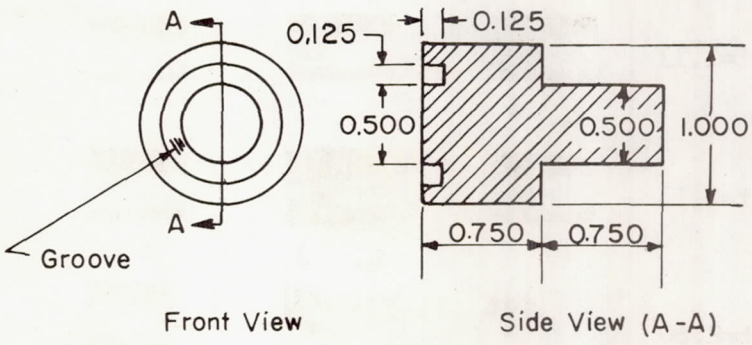

Model 32

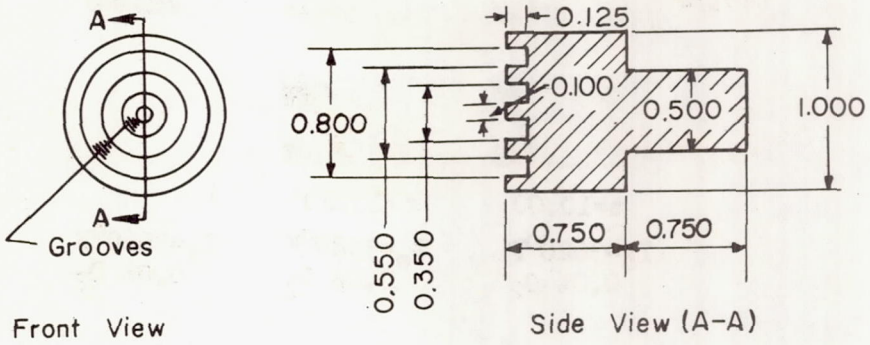

Model 33

(a) Sketches of models.

Figure 10.- Behavior of three mild-steel flat-face cylinders in chemical jet.

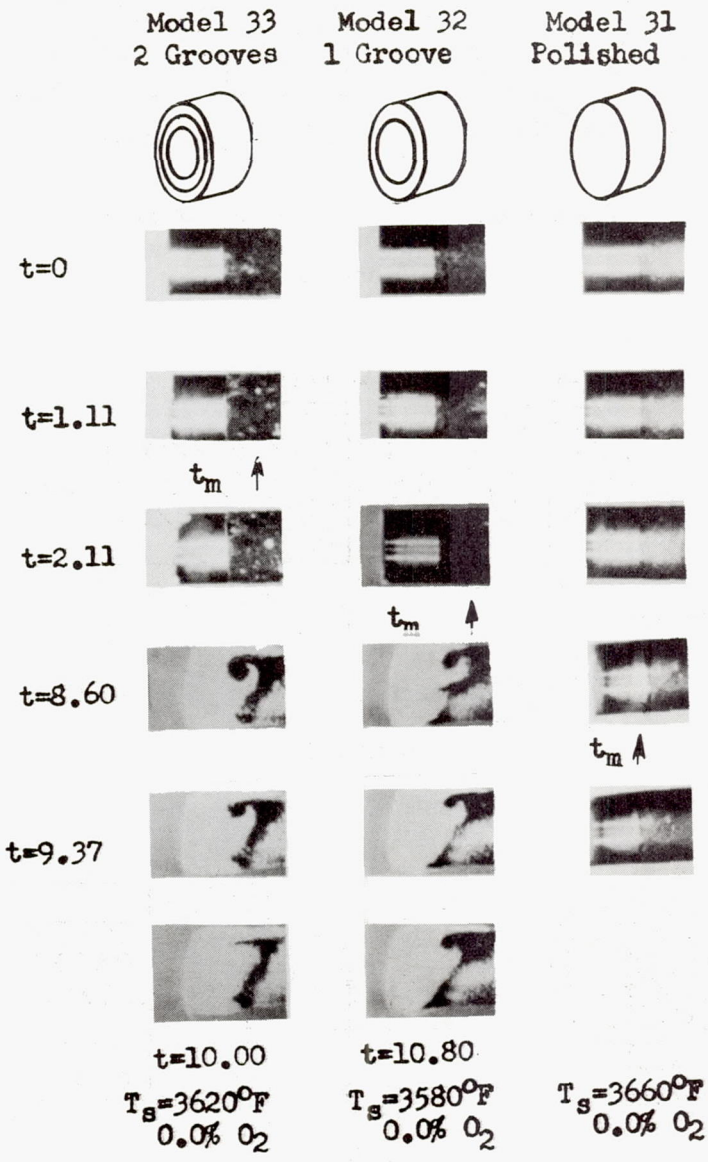

(b) Test results. L-57-130

Figure 10.- Concluded.

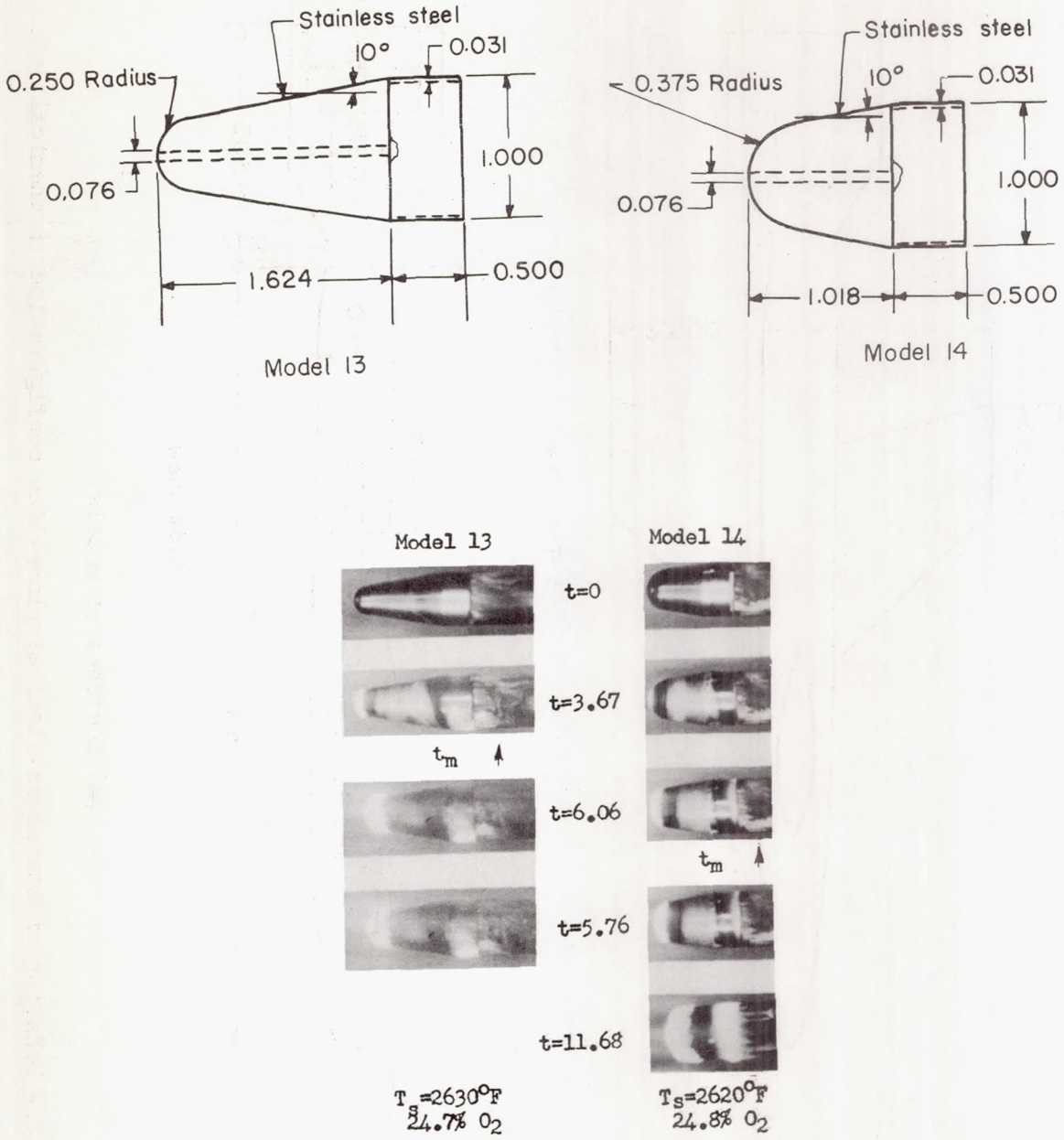

L-57-4432

Figure 11.- Behavior of stainless-steel cones in chemical jet.

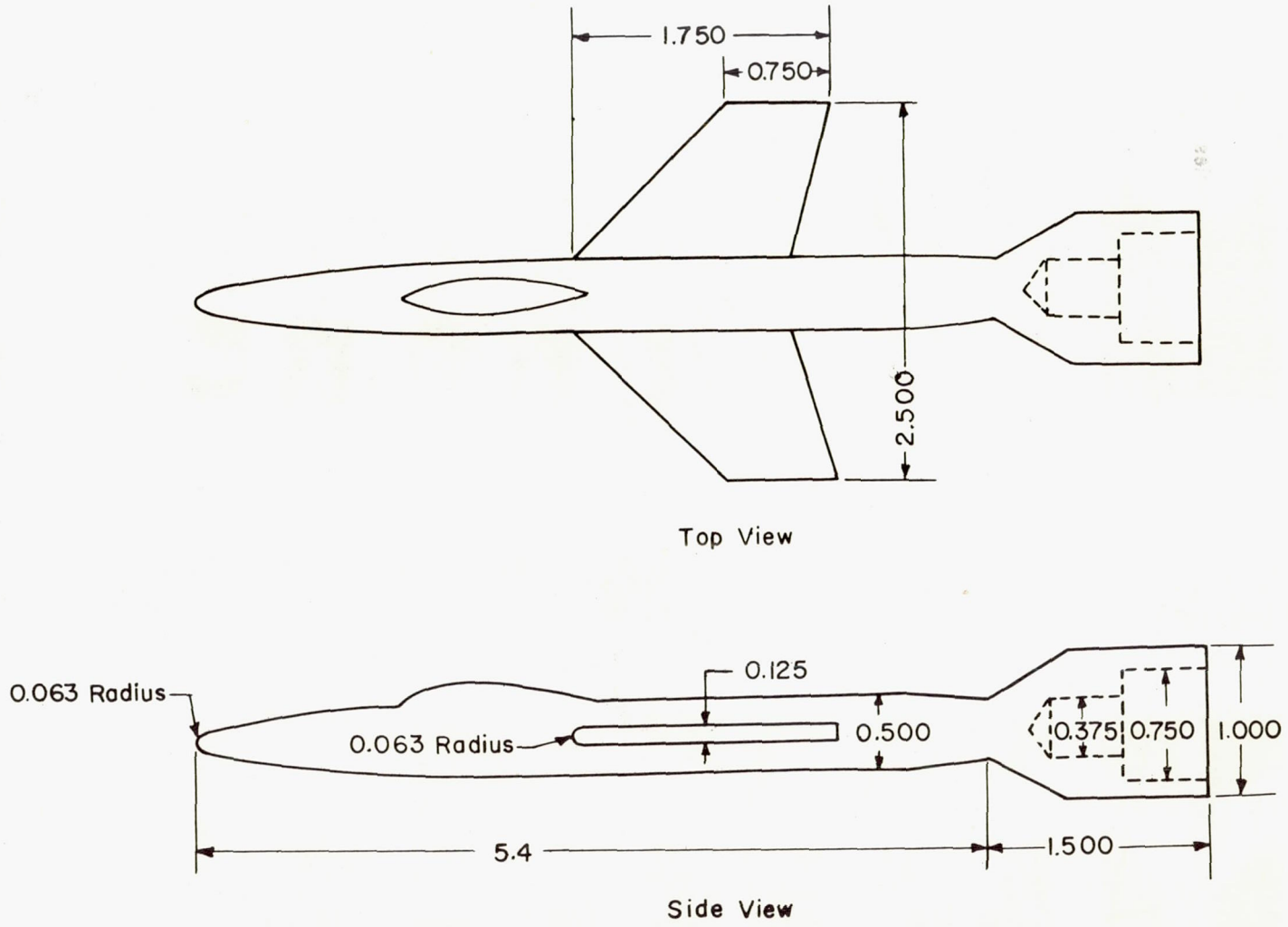

(a) Sketches of models.

Figure 12.- Behavior of stainless-steel airplane-like configuration in chemical jet.

Model 26

Model 27

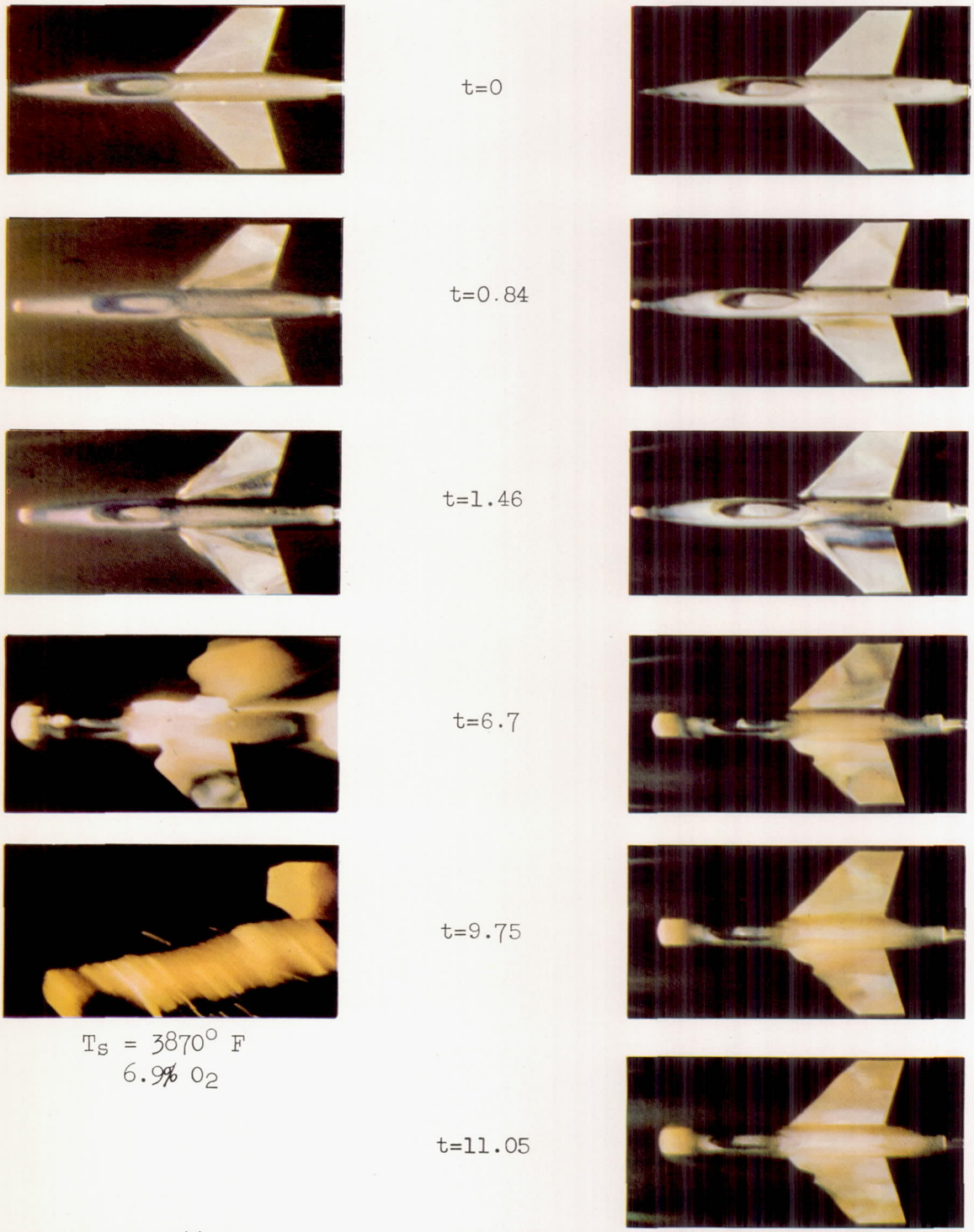

T_s = 3870° F
6.9% O_2

L-57-4431

T_s = 4190° F
1.9% O_2

(b) Test results.

Figure 12.- Concluded.

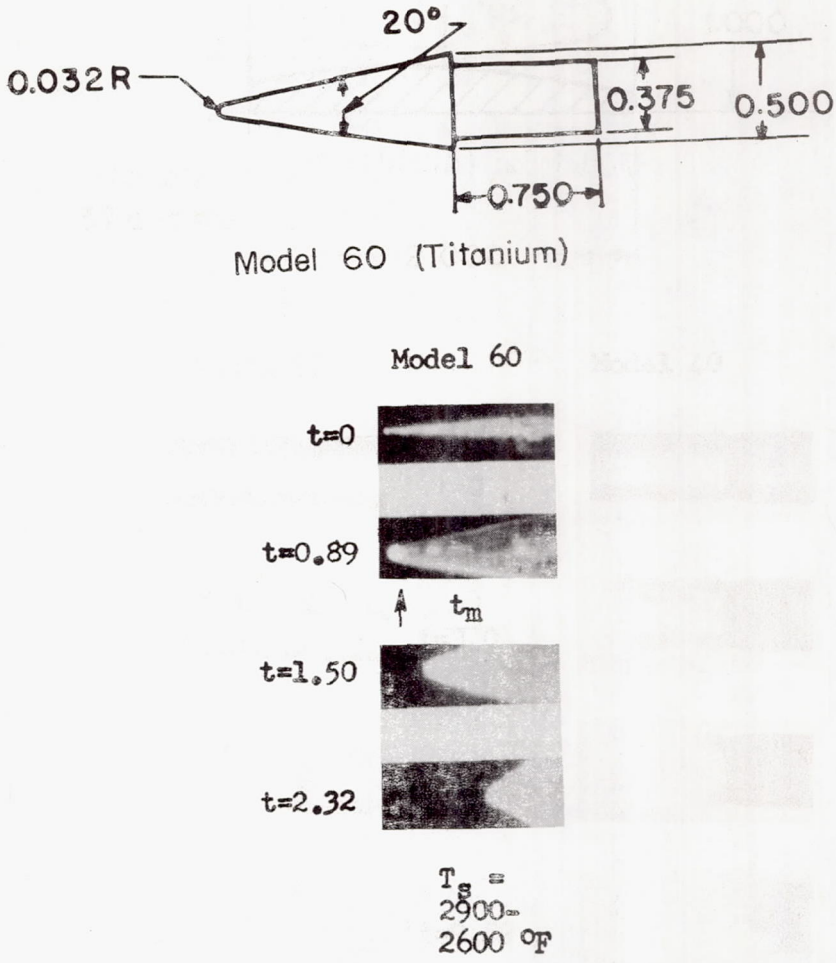

Figure 13.- Behavior of titanium in hot-air jet. L-57-4433

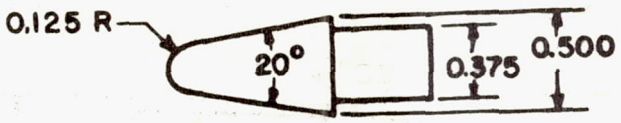

Model 52 (Aluminum)

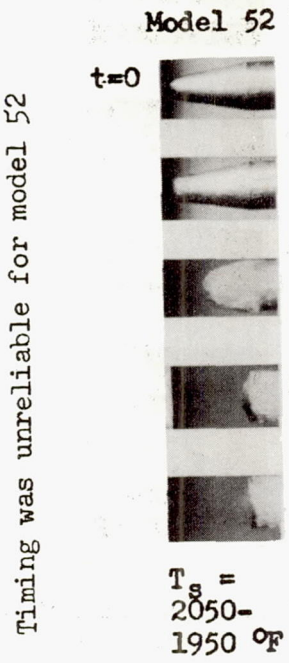

Figure 14.- Behavior of aluminum alloy in hot-air jet.

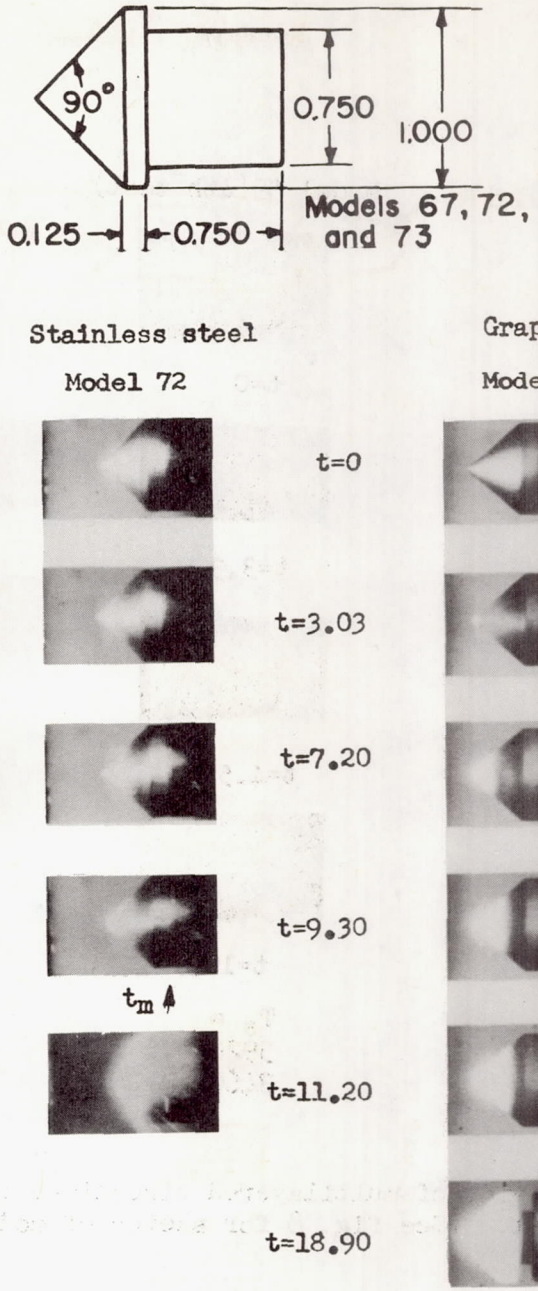

L-57-4435

Figure 15.- Behavior of mild steel, stainless steel, and graphite in hot-air jet.

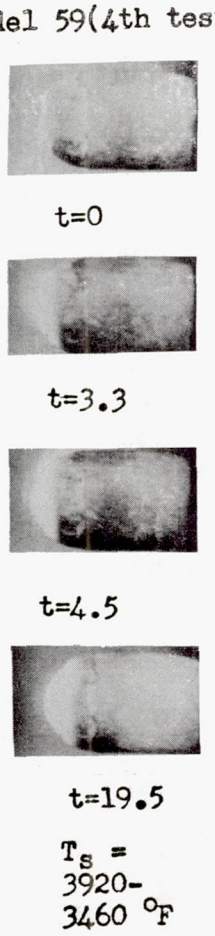

L-57-4436

Figure 16.- Behavior of multilayered zirconia-molybdenum in hot-air jet. (See fig. 8 for sketch of model.)

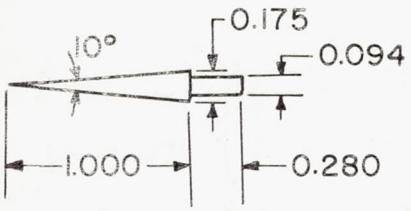

Model 74

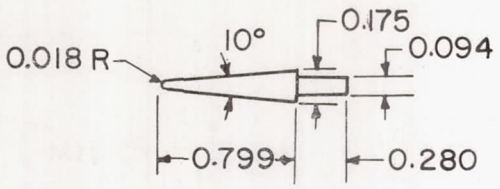

Model 75

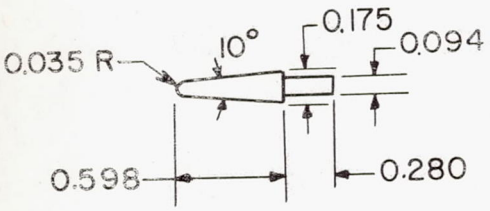

Model 76

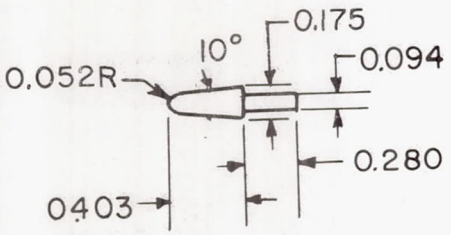

Model 77

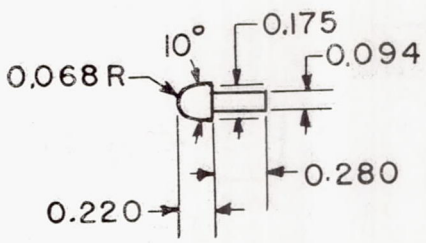

Model 78

(a) Sketches of models.

Figure 17.- Behavior of magnesium in hot-air jet.

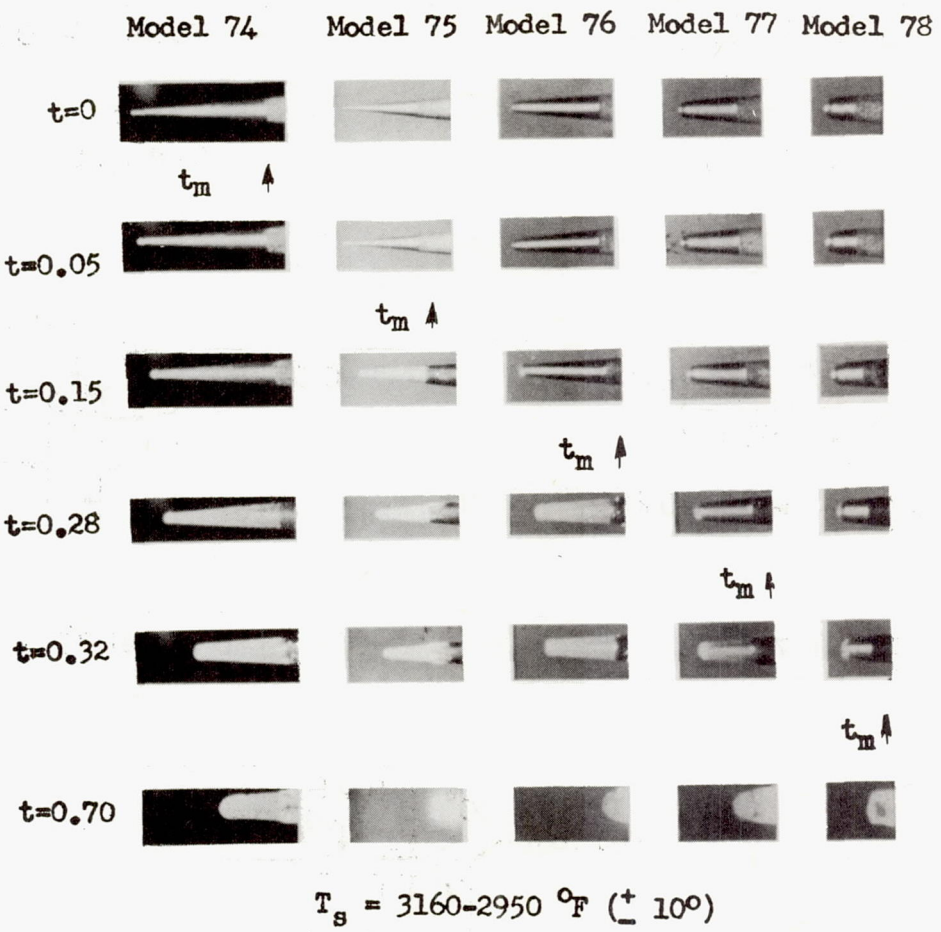

(b) Test results. L-57-141

Figure 17.- Concluded.

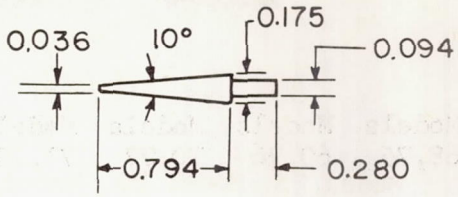

Model 68

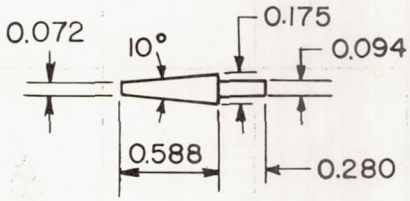

Model 69

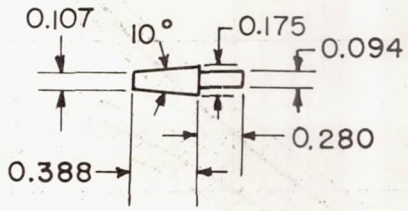

Model 70

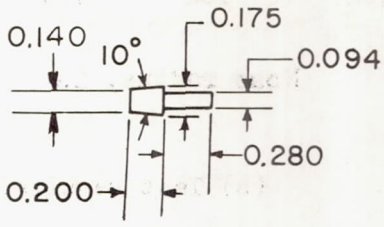

Model 71

(a) Sketches of flat-face models. (See fig. 17 for sketches of hemisphere-face models.)

Figure 18.- Behavior of magnesium cones in hot-air jet at stagnation temperatures of approximately 3,160° F to 2,950° F.

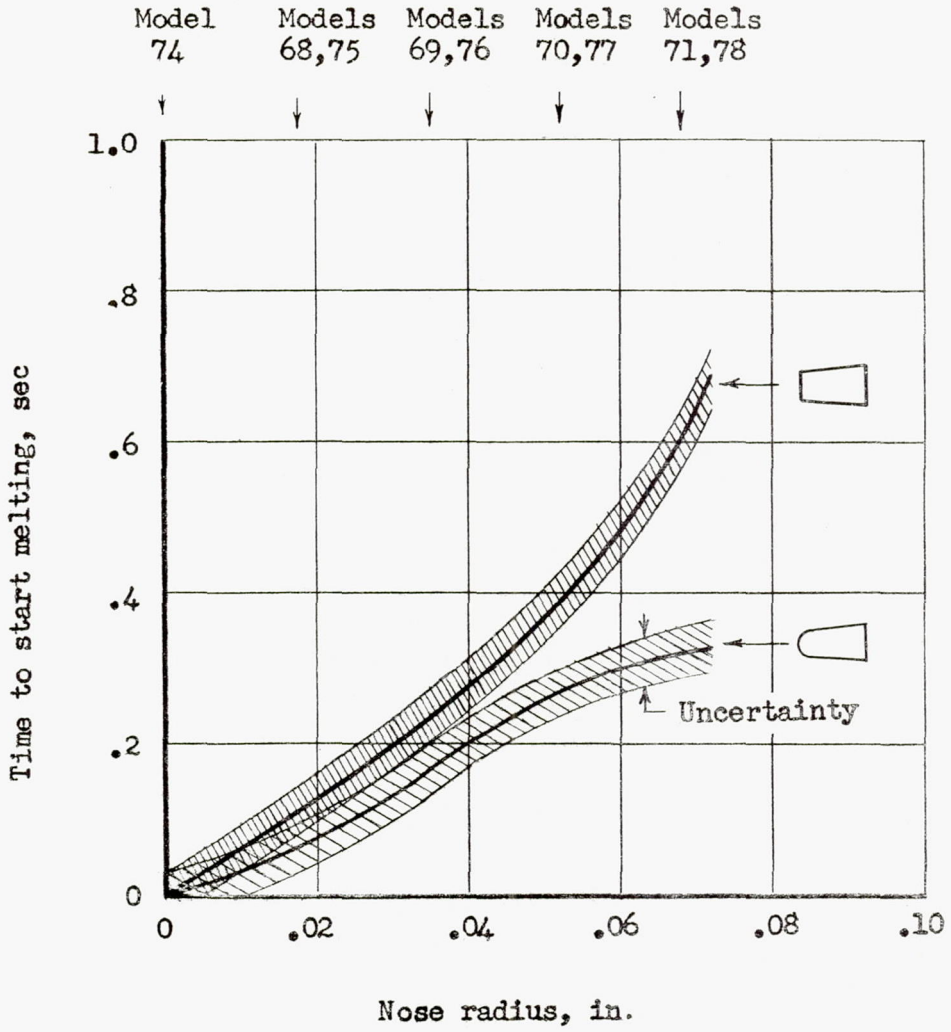

(b) Test results.

Figure 18.- Concluded.

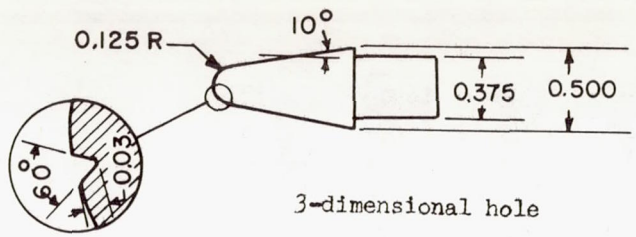

Model 62

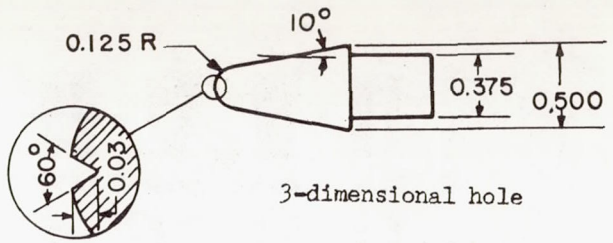

Model 64

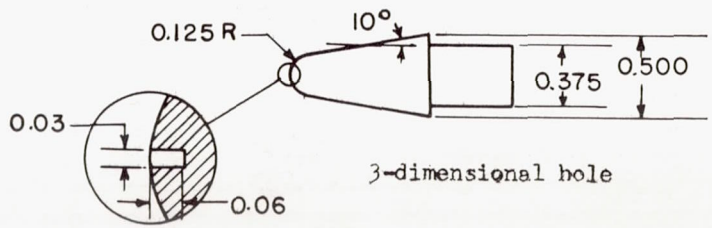

Model 63

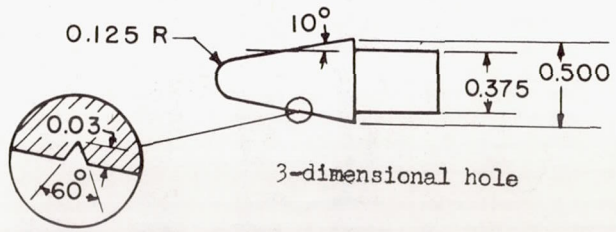

Model 65

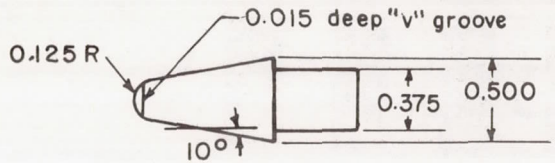

Model 66

(a) Sketches of models.

Figure 19.- Behavior of mild-steel hemisphere-face cones, with holes and grooves, in hot-air jet.

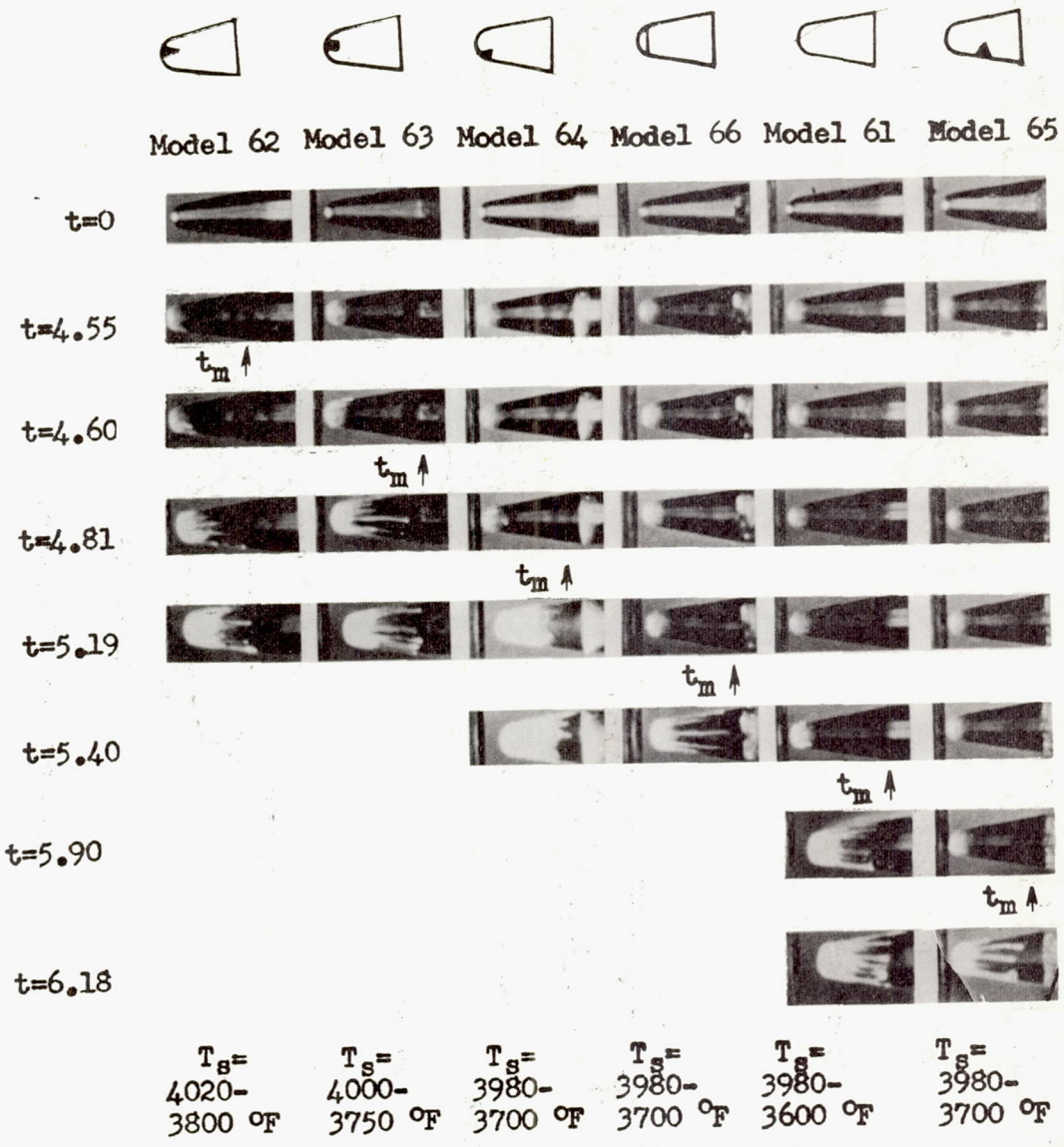

(b) Test results. L-57-142

Figure 19.- Concluded.

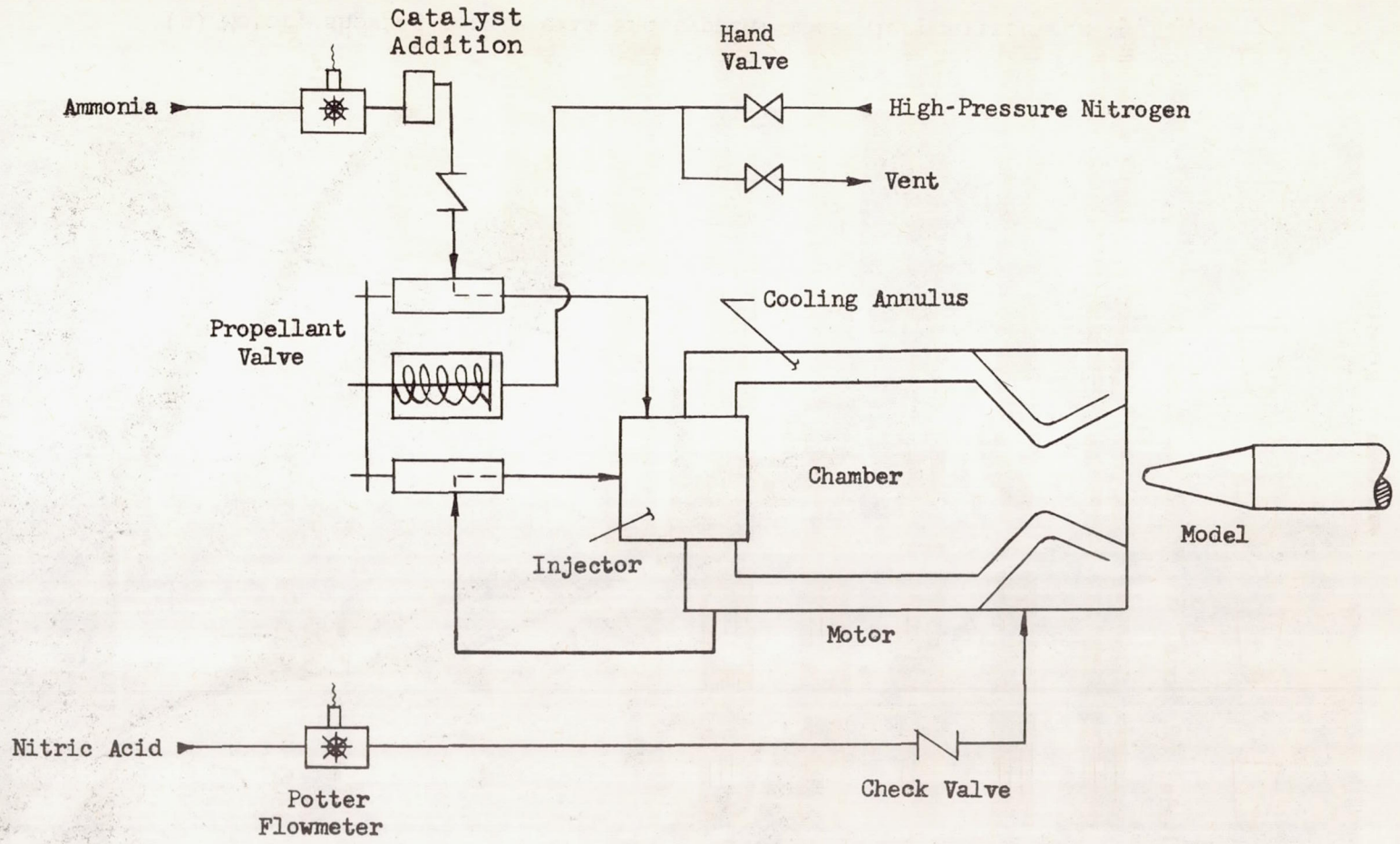

(a) Simplified flow diagram.

Figure 20.- Supersonic chemical jet.

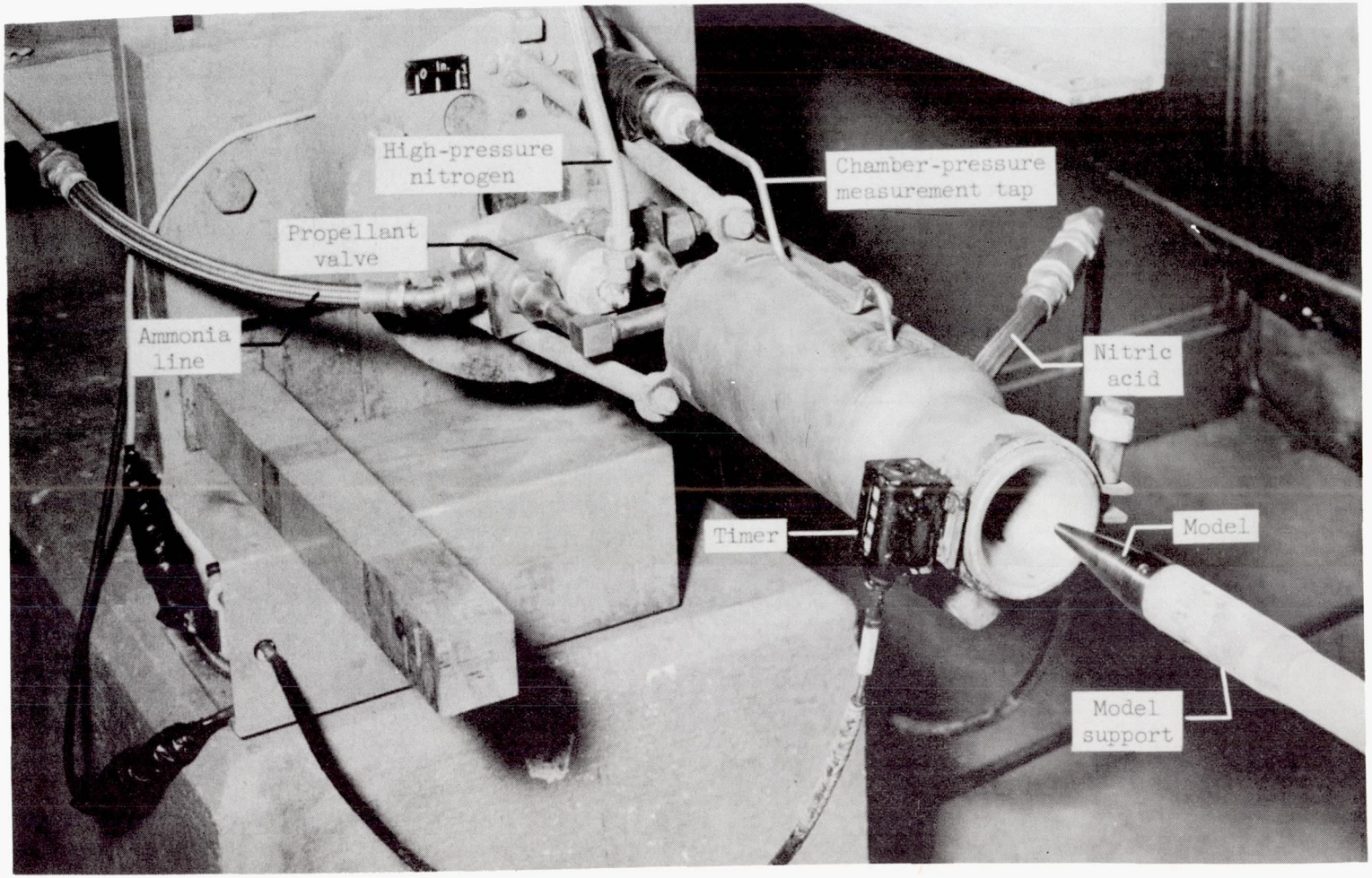

L-93090.2

(b) Motor, showing nozzle exit and typical model in position for testing.

Figure 20.- Concluded.

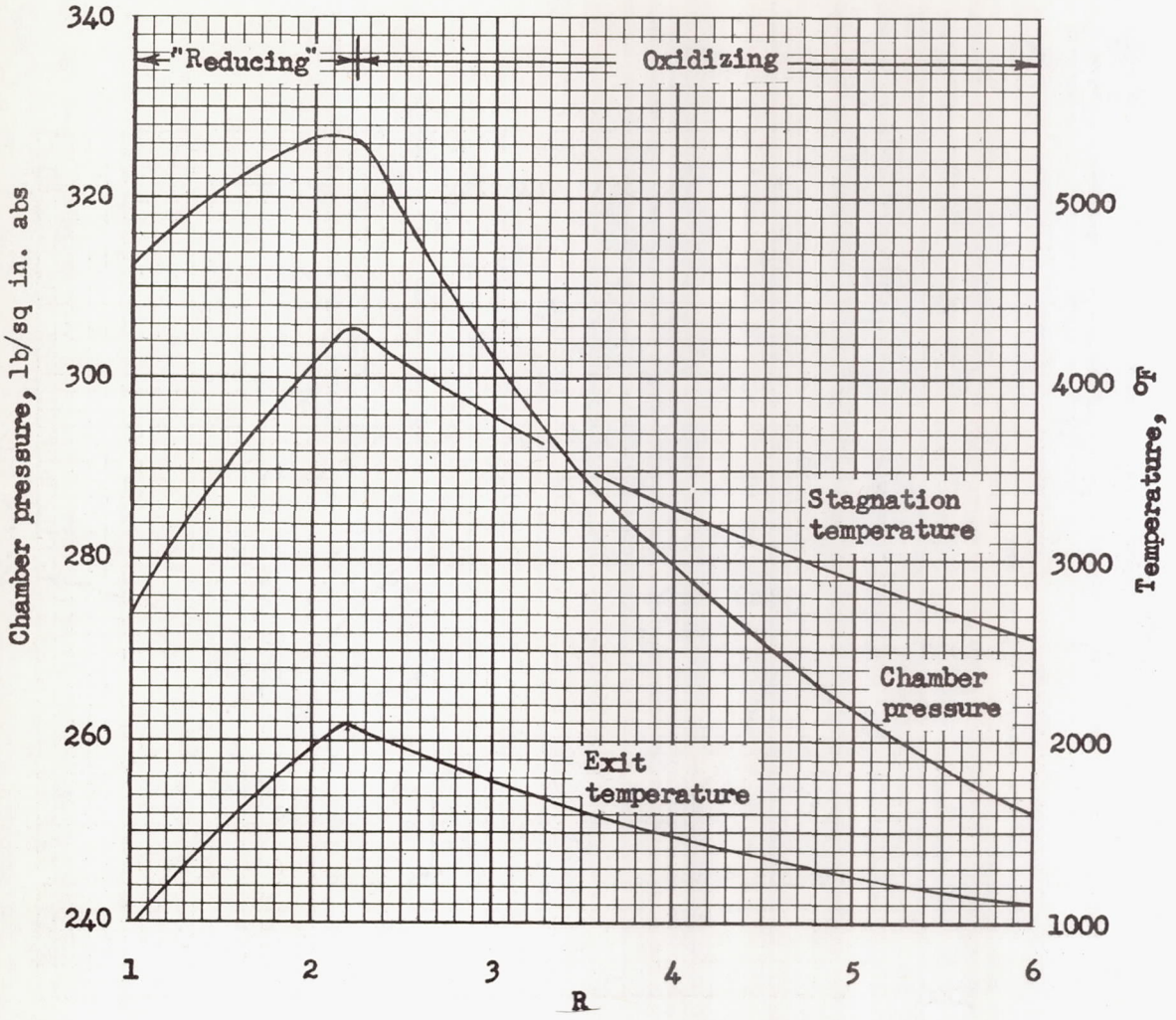

(a) Temperature and chamber pressure for weight flow rate $\dot{m}$ of 1.80 lb/sec.

Figure 21.- Theoretical chemical-jet flow parameters plotted against R (weight ratio of red fuming nitric acid (14 percent nitrogen dioxide) to ammonia), for nozzle having a throat area of 0.887 square inch and exit area of 3.46 square inches.

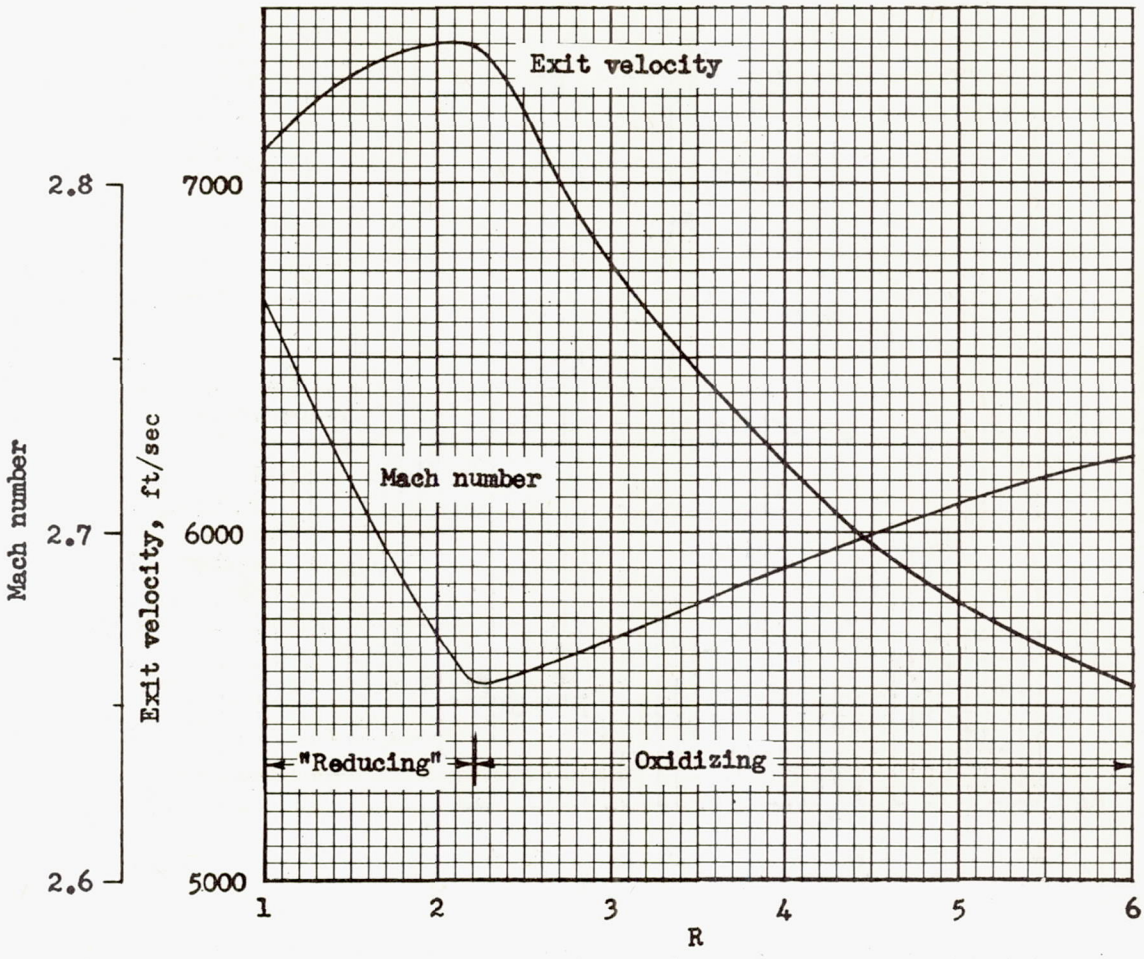

(b) Exit velocity and Mach number for weight flow rate $\dot{m}$ of 1.80 lb/sec.

Figure 21.- Continued.

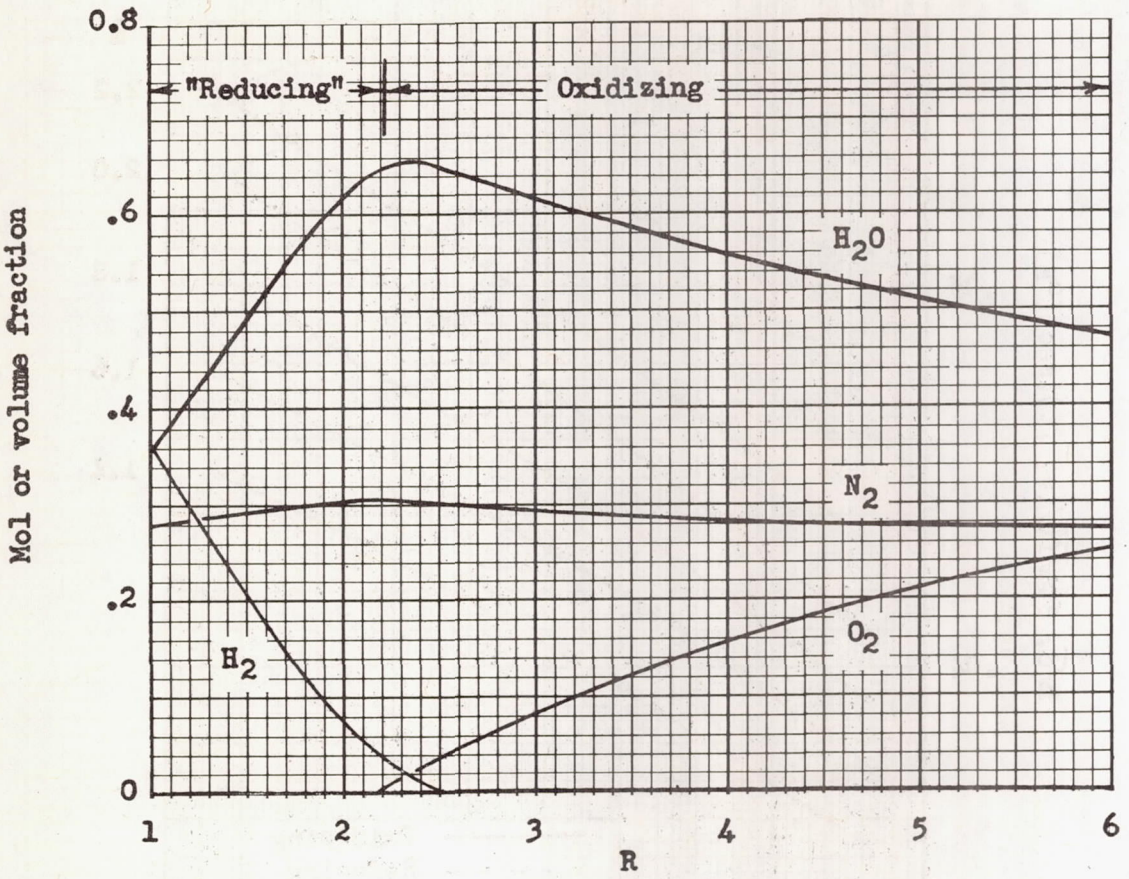

(c) Exhaust gas composition (major products) for constant-composition expansion from chamber pressure of 300 lb/sq in. abs.

Figure 21.- Concluded.

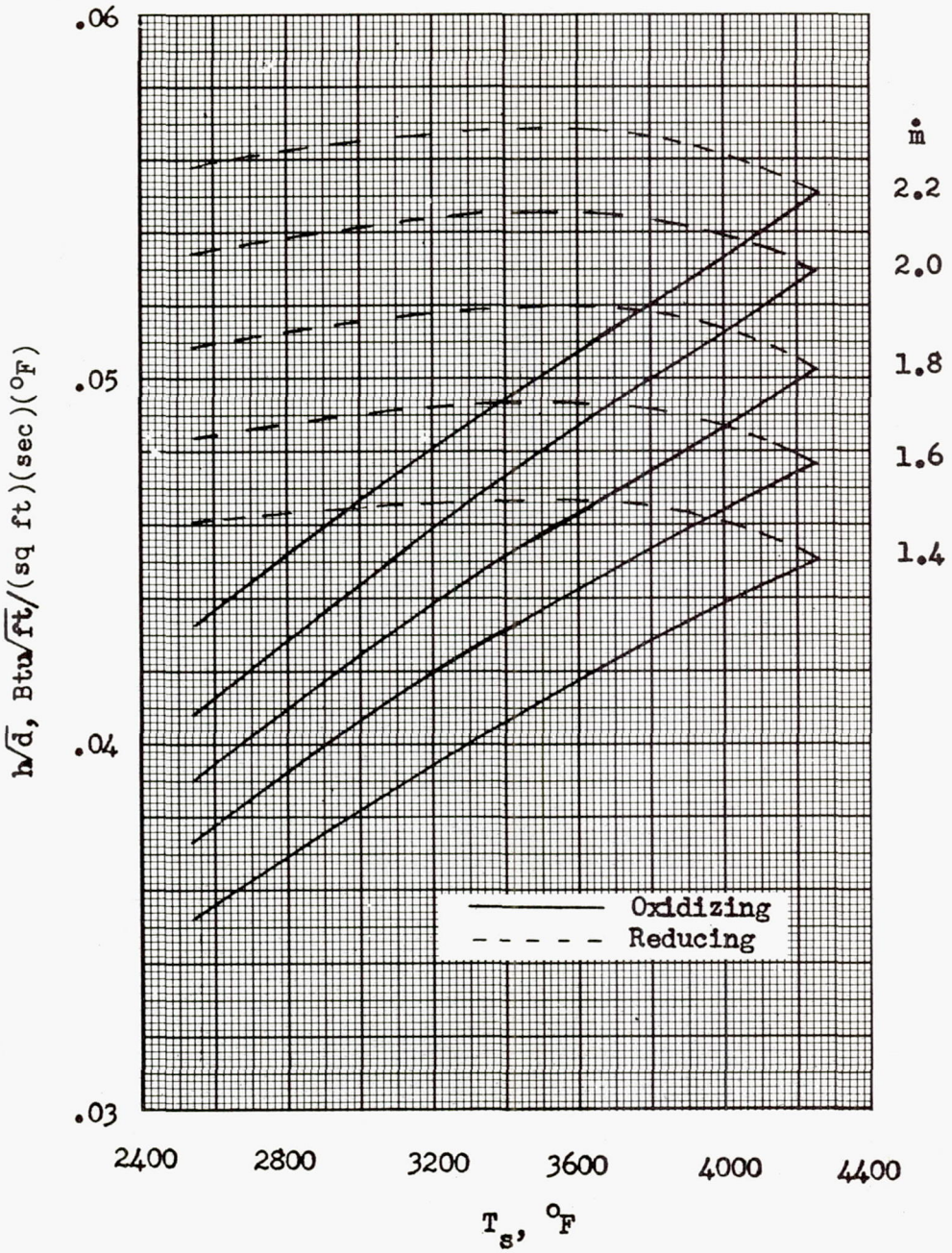

Figure 22.- Chemical-jet stagnation-point heat-transfer parameter plotted against stagnation temperature for various mass flow rates.

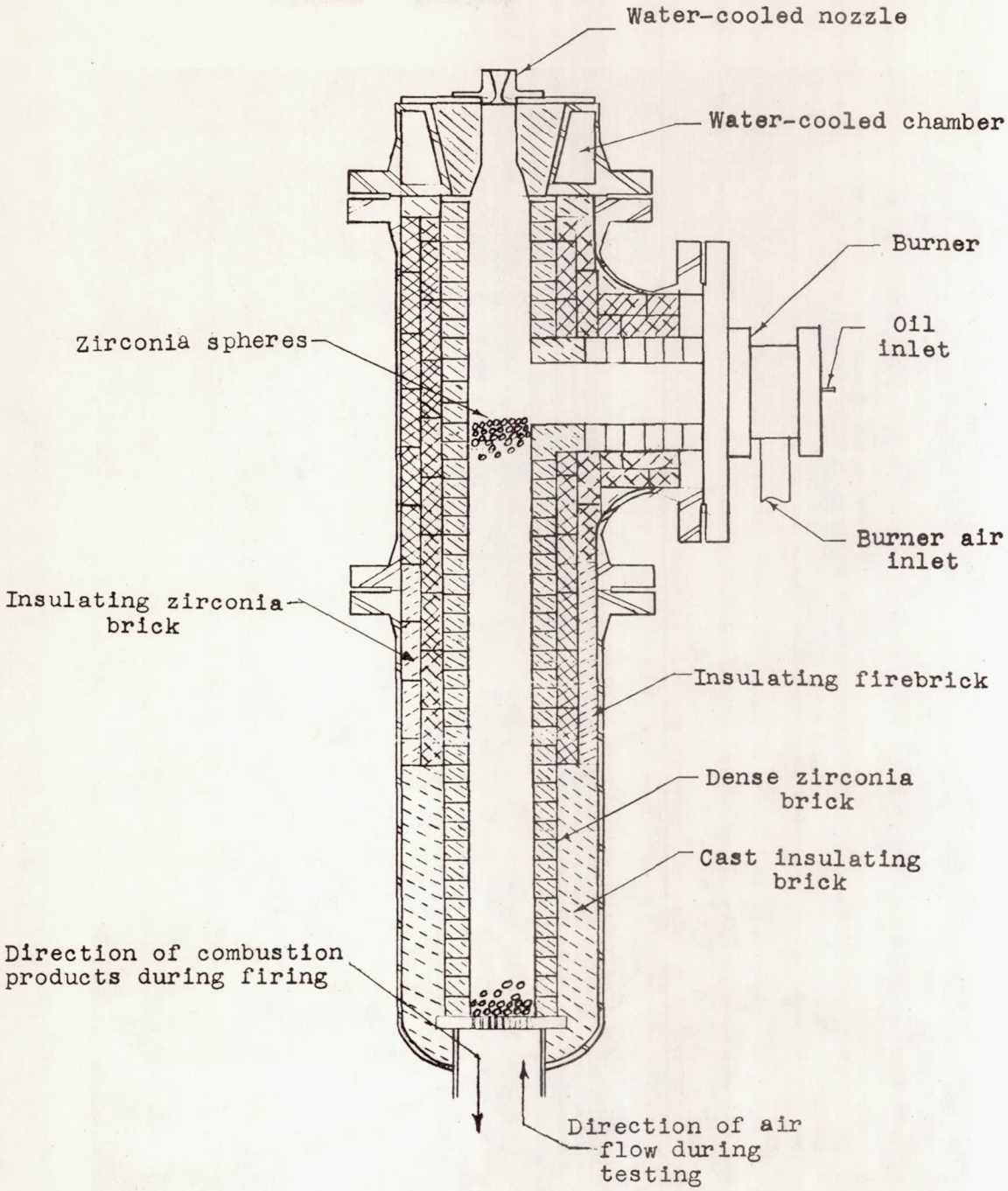

(a) Cross-section sketch.

Figure 23.- Ceramic-heated jet (laboratory model); referred to as hot-air jet in present report.

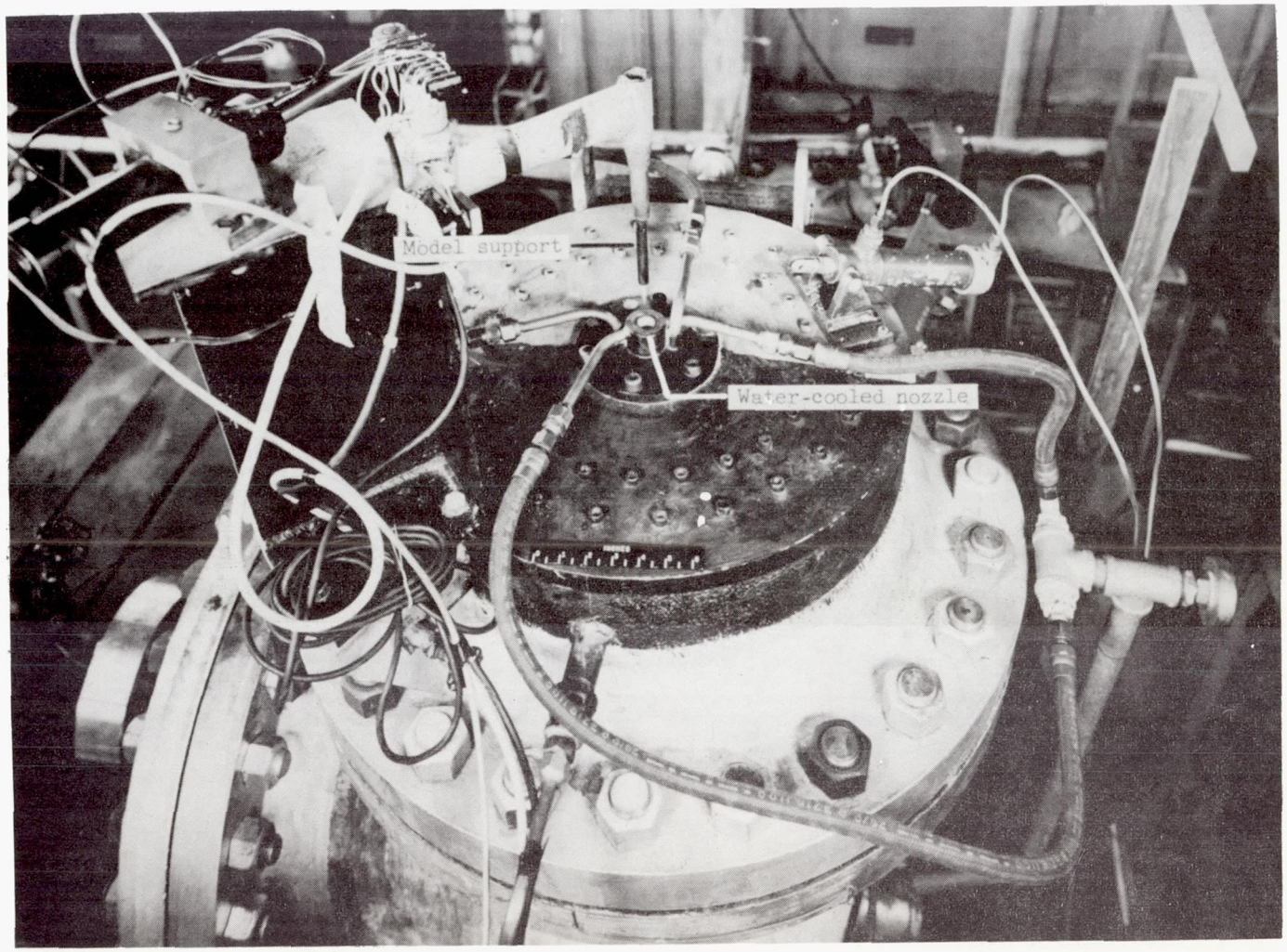

(b) Nozzle exit and typical model in testing position. L-95216.1

Figure 23.- Continued.

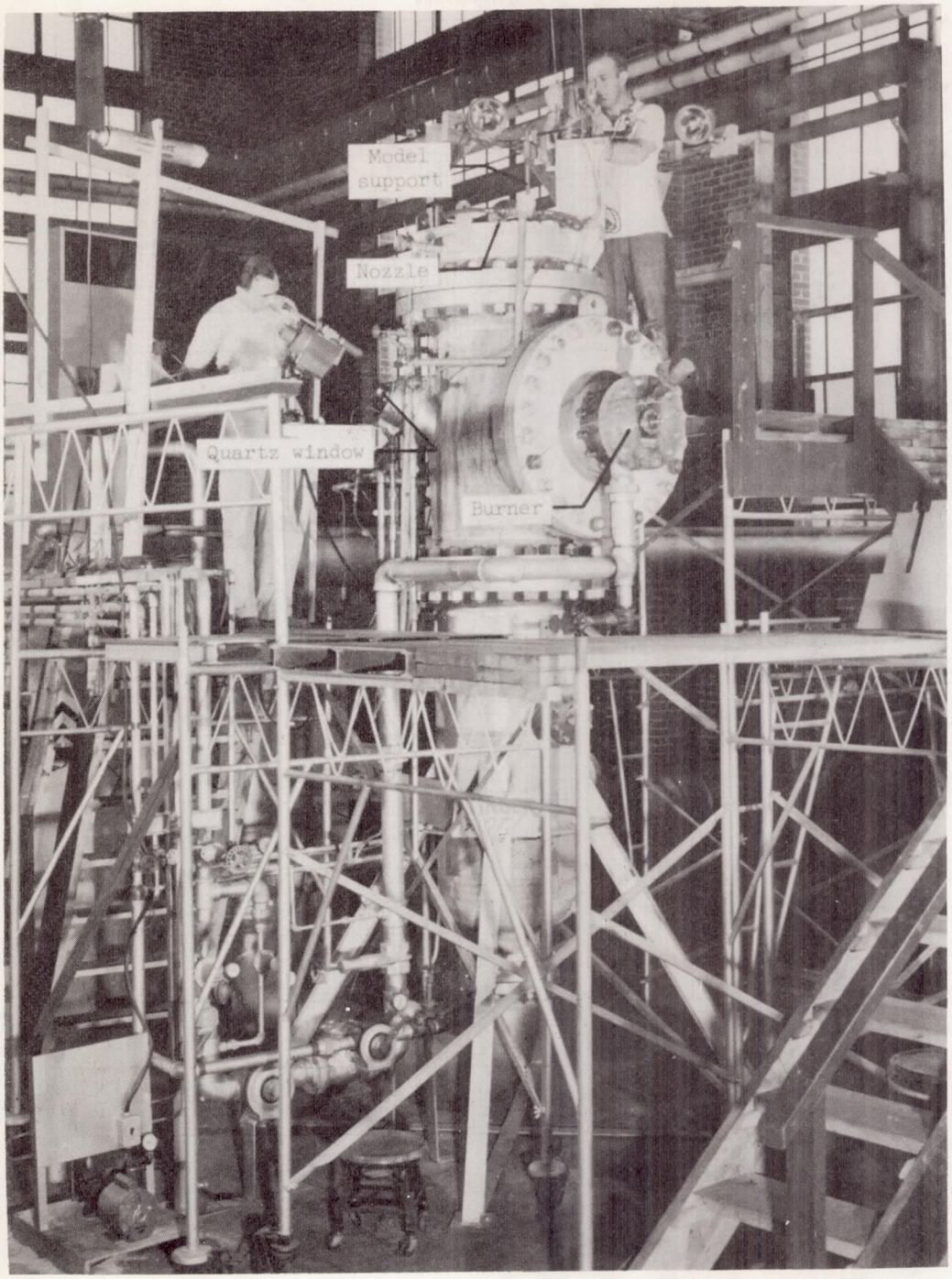

(c) Overall view. L-95214.1

Figure 23.- Concluded.

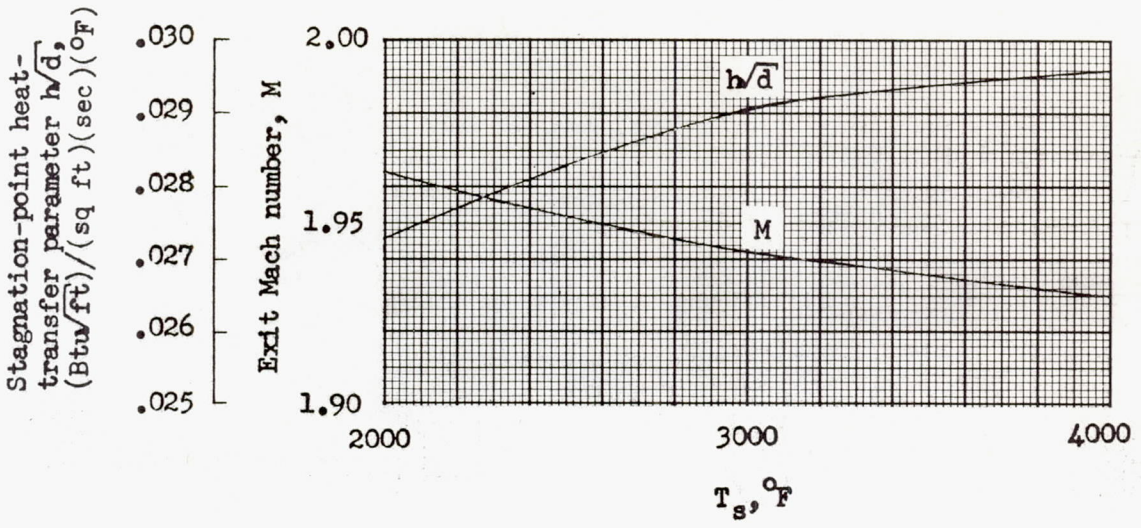

(a) Mach number and stagnation-point heat-transfer parameter.

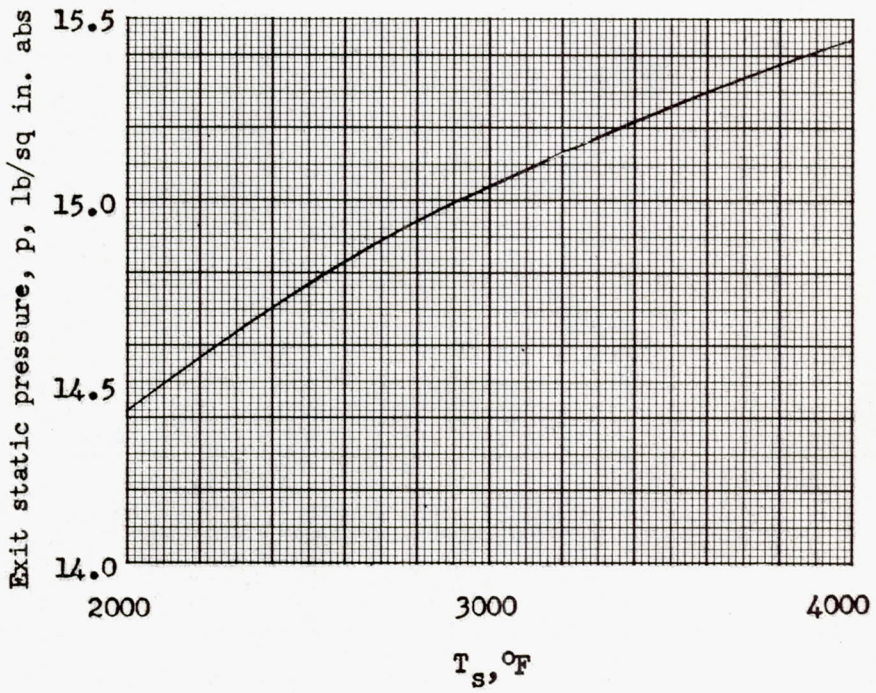

(b) Static pressure.

Figure 24.- Theoretical flow parameters for ceramic-heated jet (hot-air jet) for a stagnation pressure of 105 lb/sq in. abs.

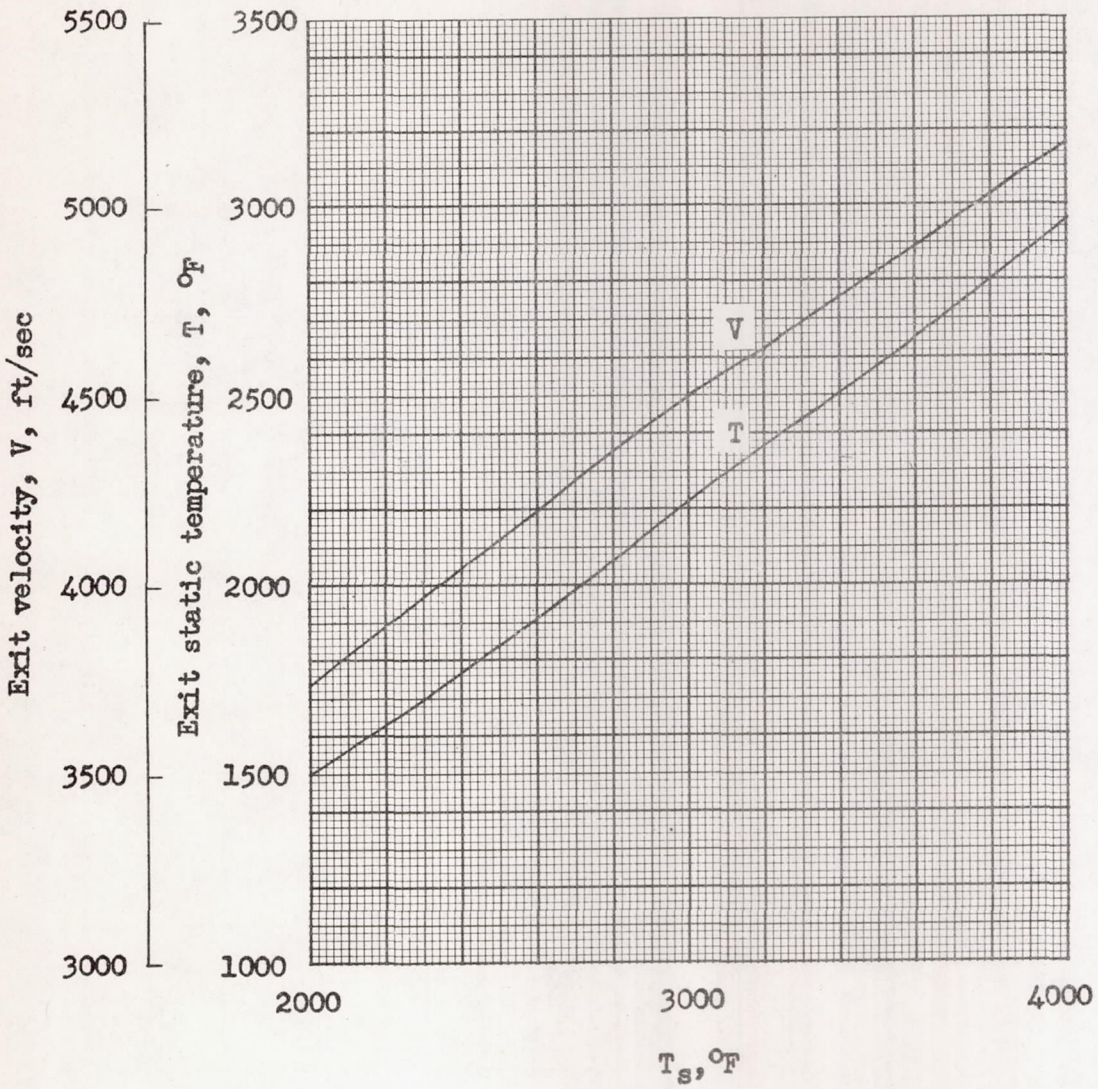

(c) Velocity and static temperature.

Figure 24.- Concluded.